MULTIBODY DYNAMICS 2007, ECCOMAS Thematic Conference
A. Mohan, S.K. Saha
Milano, Italy, 25–28 June 2007

A COMPUTATIONALLY EFFICIENT AND NUMERICALLY STABLE SIMULATION ALGORITHM FOR SERIAL ROBOTS WITH FLEXIBLE LINKS

Ashish Mohan[*] and S. K. Saha[†]

Department of Mechanical Engineering
Indian Institute of Technology Delhi, New Delhi, India

[*]presently with Hi-Tech Roboticz Systems Limited, Gurgaon, India
email: ashishsept13@rediffmail.com
[†]presently with Indian Institute of Technology Madras, Channai, India
email: saha@mech.iitd.ac.in

Keywords: Flexible, Forward dynamics, DeNOC, Computational complexity, Stability.
Abstract. *A methodology for the formulation of dynamic equations of motion of a serial flexible-link manipulator using the decoupled natural orthogonal complement (DeNOC) matrices, introduced elsewhere for rigid links, is presented in this paper. First, the Euler Lagrange (EL) equations of motion of the system at hand are written. Then, using the DeNOC matrices associated with the velocity constraints of the connecting bodies a set of recursive expressions for the elements of the associated matrices and vectors are obtained. The expressions also allow one to obtain a recursive forward dynamics algorithm not only for rigid link manipulators, as reported earlier, but also for the flexible link manipulators. In contrast to a serial-chain robot with n rigid links which can have O(n) forward dynamics algorithm, the one proposed here for the n flexible link has an order of $O(n)+O(m^3/3)$ — m being the maximum number of modes considered for the modeling of beam deflections — complexity. Simulation results for the 3-link Canadarm, considering all its links flexible are reported here, using the proposed algorithm. The numerical stability and efficiency of the proposed algorithm are also investigated, with respect to the Canadarm.*

1 INTRODUCTION

Research on robotic systems with flexible links started in the international arena in early 1970s. A comprehensive review of various techniques on the modeling of robot-link flexibility is given in [1]. The techniques are principally distinguished as Euler-Lagrange (EL) and Newton-Euler (NE) formulations. The EL formulation requires the successive differentiation of the Lagrangian function of the kinetic and potential energies of the system at hand. Such differentiations are very complex for large multibody systems. Hence, researchers tend to avoid this approach to develop efficient algorithms. As a result, many efficient algorithms for robot dynamics are based on the NE formulation, as given in [2], and others. However, as shown in [3] for rigid-link robots, there is no fundamental difference in the computational complexity of the algorithms based on the EL and NE formulations. The computational efficiency using the NE formulation is apparently visible due the recursive structure in the associated expressions. Hence, the NE formulations are generally preferred by the researchers. Besides the appropriate choice of dynamic formulation methodology, viz. EL or NE, to achieve better computational efficiency of a flexible link robot, selection of proper kinematic model to express the link deflection is also very crucial. Different researchers have used different methods for the kinematic description of the link deflection. The most common of which are lumped parameters [4], finite element method (FEM), and the assumed mode method (AMM) [5-7]. The lumped parameter method is generally not preferred by the researchers because elastic deflections of only very small magnitude can be modeled accurately using this technique. Comprehensive comparisons of the other two methods viz., FEM and AMM, and the computational efficiency and stability of the simulation algorithms using formulation based on them is done in [6-8]. Between the two, namely FEM and AMM, the latter is preferred in serial robotic applications where each link is treated as flexible slender beam. In FEM, more than one element are required in order to obtain an acceptable approximation of a particular frequency which leads to the introduction of extra nodal coordinates, along with high and spurious frequencies. This increases the dimensionality of the state variables and the numerical noise [8], which detrimentally affects the overall computational efficiency of the algorithm. In contrast, using a specific number of eigen functions, in AMM, exact reproduction of corresponding natural frequency is assured. Hence, although efficient dynamic models based on FEM approach are present in the literature [9], AMM is preferred by researchers to develop recursive and efficient algorithms for robots with flexible links [5, 10-12].

Book [5] developed a non-linear recursive dynamic formulation for flexible manipulators connected through revolute joints. Based on similar kinematic modeling technique, Kim and Haug [13] presented a recursive method based on variational vector calculus. The dynamic model of deformable bodies using the NE approach is also given by Shabana [14]. The combination of the AMM and the Ritz vectors form another efficient and accurate vector bases for the modeling of flexible bodies. De Luca and Siciliano [12], on the other hand, have given analytical closed form equations of motion for the planar lightweight robot arms with multiple flexible links, and provided extensive simulation results.

In this paper, we present an alternative dynamic modeling technique based on the equivalence of EL and NE formulation, and the use of decoupled natural orthogonal complement (DeNOC) matrices. We then present a recursive algorithm for the forward dynamics (FD) of a serial flexible link manipulator. The order of the proposed algorithm is $O(n)+O(m^3/3)$, where n is the total number of links and m is the maximum number of modes in which the flexible links of a robot are assumed to vibrate. The proposed FD algorithm is possible due to the analytical $\boldsymbol{UDU}^T$ decomposition of the generalized inertia matrix (GIM) associated with the system's dynamic equations of motion, where $\boldsymbol{U}$ and $\boldsymbol{D}$ are respectively the upper block triangle and block diagonal matrices. The proposed analytical decomposition

is very similar to the conventional Cholesky decomposition [15] carried out to solve the joint accelerations required in FD. The difference is that, in the proposed methodology, one writes the elements of the GIM as expressions instead of computing them as numbers in the conventional approach. As a result, when the Gaussian rules are applied on the analytical expressions of the elements of the GIM, followed by the backward and forward substitutions [15] to solve for the joint accelerations, elegant recursive expressions are exposed, which are not explicit when done numerically. Hence, the conventional approach leads to $O\left[\frac{(n+m)^3}{3}\right]$ FD algorithm, whereas the proposed algorithm has $O(n)+ O(m^3/3)$, complexity, where $O(m^3/3)$ complexity is caused due to those terms in the GIM associated with the link flexibility. The scalar elements in the sub matrices of the GIM corresponding to the link flexibility cannot be expressed recursively. Hence, those $m \times n$ sub matrices have to be treated as a whole resulting in $O(m^3/3)$ complexity. Since the key step in obtaining recursive algorithm is the availability of the GIM block elements as expressions, they are obtained here using DeNOC matrices, associated with the flexible link manipulator under study. The concept of DeNOC has been originally introduced in [16] for the $O(n)$ FD algorithm for serial manipulator system. Note here that for rigid-link manipulator, there is no flexible term. Hence,, the block terms of GIM in the case of flexible-link manipulator reduces to a scalar term which have recursive relation. As a result, the complexity of the FD algorithm for a rigid link manipulator is $O(n)$ as m=0. An orthogonal complement is defined as the matrix whose columns span the null-space of the velocity constraint matrix. Hence, the premultiplication of its transpose with the unconstrained dynamic equations of motion vanishes the constrained moments and forces. As a result, a set of independent dynamic equations of motion, which are Ordinary Differential Equations (ODE), is obtained which are known to provide numerically more stable algorithms compared to the Differential Algebraic Equations (DAE) representing the same system dynamics [17]. The said orthogonal complement is, however, not unique. In some approaches, an orthogonal complement is found using schemes which are numerically more intensive requiring, for example, singular value decomposition or eigen value computations. Angeles and Lee [18] have obtained the complement for the serial rigid multibody systems naturally from the velocity constraint expressions without any complex computations. Therefore, the complement is called the natural orthogonal complement (NOC). Cyril [11] has obtained the NOC for the flexible serial robotic systems and reported a non-recursive forward dynamic algorithm. In this present work, we explored if the NOC for a serial flexible robot can be obtained in decoupled form, as done for the rigid systems in [16, 19], in order to develop a recursive FD algorithm or not. The outcome is encouraging. The proposed algorithm is not only computationally efficient but also numerically more stable.

Earlier, the use of the DeNOC for the dynamic modeling of rigid serial [19], parallel [20, 21], and closed loop [22] systems, is found to be advantageous due to following reasons: 1) Many physical interpretations like the twist propagation matrix, joint propagation vector, mass matrices for the composite and articulated bodies, etc,; 2) Complete analytical inversion of the GIM [16], which is not possible by the approaches of many existing recursive FD algorithms, e.g., [23] and others; 3) Complete ODE formulation of the parallel systems, leading to recursive FD algorithm, which was never possible using other approaches; 4) Modular and parallel algorithms [21]; and 5) Maximally recursive dynamics algorithm for the evaluation of constraint forces in a general multi-closed-loop system [22].

In this paper, extension and application of the DeNOC matrices to the serial robotic systems with all flexible links is presented. A recursive, computationally efficient and numerically stable FD algorithm for flexible robots is presented. Physical interpretations of many terms, e.g., the mass matrix of a composite flexible body, wrench inertia matrix for flexible link systems, etc. are also presented. Besides the computational efficiency, numerical

stability of the proposed forward dynamic algorithm for the flexible link robotic systems are also studied. It is pointed out here that simulation, is a two step process, namely, (1) the computation of the generalized accelerations from the equations of motion of a system at hand for the given actuator forces and torques; and (2) numerical integration of the accelerations computed in step (1) to obtain the corresponding rates and positions. Thus, the nature of simulation results depends as much on the FD algorithm as on the integrator used in step (2). The role of integrator's algorithm, as well as the FD scheme, is very crucial in determining the stability characteristics of the simulation results. While working with low-order, linear models, resulting from simpler systems, computers are usually insensitive to numerical difficulties, and the common mathematical software tools like MATLAB, etc. give accurate results. However, dynamic models of the flexible robots are a set of highly coupled and non-linear equations and the finite-precision arithmetic of a computer is not so forgiving. Hence, it is essential to exercise caution to restrict the cumulative growth of errors, through appropriate choice of the FD algorithm and the numerical integrator. Hence, it is possible that the simulation results of a system are unstable even if the real system is stable. This phenomenon of instability in the simulation results due to the effect of the FD algorithm, irrespective of the numerical integrator used in step (2), is attributed to how a FD algorithm works. A FD algorithm is thus numerically stable if it does not introduce any additional sensitivity than that already inherent in the problem due to its physical characteristics and caused due to the integrator. Various methods, namely based on the drift in the total energy of the system, formulation stiffness phenomenon, etc. have been used by the researchers for investigating the numerical stability aspects [8, 24-26]. However, most of the study on stability of numerical algorithms, is limited to the rigid robotic systems. The effect of flexibility of links on the numerical aspects of FD algorithms still remains a relatively less explored area. In this paper, two schemes: one based on conservation of power and its drift, and the other one using the time duration for which the simulation results match the desired results, are adopted to test the stability of the proposed algorithm.

The paper is organized as follows: In Section 2, kinematic description of a flexible link is given. Some definitions are introduced in Section 3, followed by the formulation of the dynamic model in Section 4. In Section 5, a recursive algorithm for the FD of serial flexible robotic systems is proposed. The computational complexity aspects of the proposed algorithm are presented in Section 6. Simulation results to validate the proposed algorithm and its numerical stability analysis are presented in Section 7, followed by conclusions in Section 8.

2 KINEMATIC DESCRIPTION OF A FLEXIBLE LINK

Figure (1) shows a serial robotic system having a fixed base and *n*-flexible moving bodies. The i^{th} link is shown in Fig. (2). For simplicity, and without loosing any generality, each flexible link is assumed to vibrate in m^{th} bending mode. Hence, the degree of freedom (DOF) of the system is, $\bar{n} \equiv (1+3m)n$. For the kinematic description of the elastic deformation of each flexible link, the AMM [1, 5] is used. Thus, the deformation of any element $\widetilde{E}_{\boldsymbol{i}}$ lying along $\hat{X}_{\boldsymbol{i}+1}$ axis, Fig. (2), is given by the 3-dimensional vector, $\boldsymbol{u}_i$, as,

$$\boldsymbol{u}_i(\bar{a},t) \equiv \left[u_i^x(\bar{a},t) \quad u_i^y(\bar{a},t) \quad u_i^z(\bar{a},t)\right]^T \tag{1a}$$

where u_i^x , u_i^y and u_i^z are the projections of the deflection vector $\boldsymbol{u}_i$ on the $\hat{X}_{\boldsymbol{i}+1}, \hat{Y}_{\boldsymbol{i}+1}$ and $\hat{Z}_{\boldsymbol{i}+1}$ axes, respectively, and $\bar{\boldsymbol{a}}_i$ is the position vector of element $\widetilde{E}_{\boldsymbol{i}}$ from O_i'. Thus, $\bar{\boldsymbol{a}}_i = \bar{a}_i \hat{\boldsymbol{x}}_{i+1}$,where $\hat{\boldsymbol{x}}_{i+1}$ is the unit vector along $\hat{X}_{\boldsymbol{i}+1}$ axis and $\bar{a}_i$ is the axial distance of

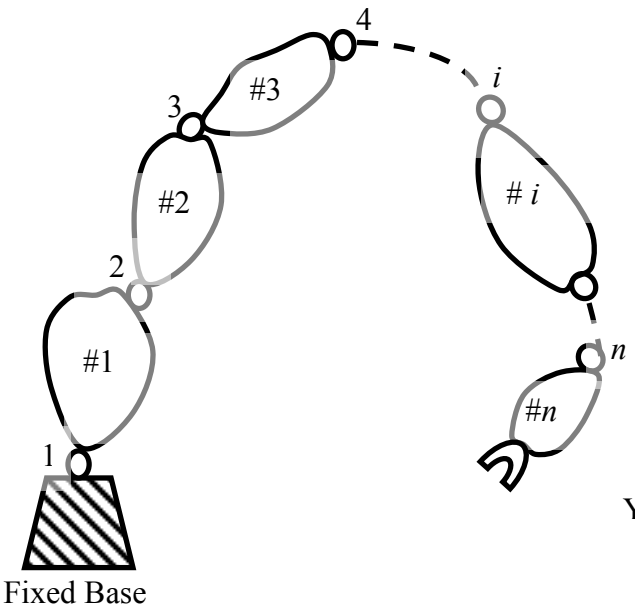

Figure 1: An n-flexible link robot

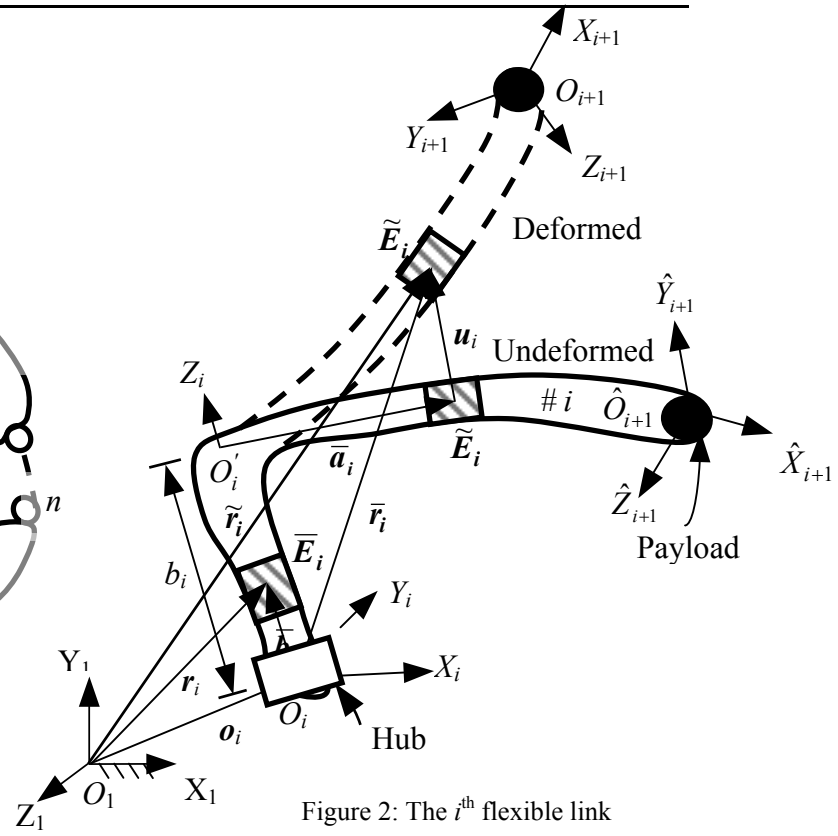

Figure 2: The i^{th} flexible link

$\widetilde{E}_i$ from O_i' along $\hat{X}_{i+1}$ of the i^{th} link. Note that $\bar{a}_i$ varies from 0 to a_i –one of the DH parameters of the link. The component u_i^x is a function of u_i^y and u_i^z, which is given by [11],

$$u_i^x \approx \frac{1}{2}\int_0^{a_i}\left[\left(\frac{\partial u_i^y}{\partial \bar{a}_i}\right)^2 - \left(\frac{\partial u_i^z}{\partial \bar{a}_i}\right)^2\right] d\bar{a}_i \tag{1b}$$

The term, u_i^x of eq. (1b), results in centrifugal stiffening of the link, which is significant in the analysis of flexible multibody systems, only when the angular rates of the bodies are considerably greater than their first natural frequency [2, 9]. Moreover, the flexibility along the joint axis, Z_i, is ignored due to the assumption of i^{th} link is rigid along Z_i, i.e., $O_i O_i'$ of Fig. (2). The above two assumptions are quite common in the literature [5-6, 11-12]. For a prismatic joint, the flexibility along the Z_i-axis is also ignored. Otherwise, the smooth translation along the axis is not possible. Now, using the AMM, the vector, $\boldsymbol{u}_i$, can be expressed in terms of space dependent eigen functions and time dependent amplitudes, as,

$$u_i^x = \begin{cases} 0 & \text{: For revolute joints} \\ \sum_{j=1}^{m_i} s_{i,j}^x d_{i,j}^x & \text{: For prismatic joints} \end{cases}$$

$$u_i^y = \sum_{j=1}^{m_i} s_{i,j}^y d_{i,j}^y \tag{1c}$$

$$u_i^z = \begin{cases} \sum_{j=1}^{m_i} s_{i,j}^z d_{i,j}^z & \text{: For revolute joints} \\ 0 & \text{: For prismatic joints} \end{cases}$$

Now, the following three $3\times m_i$ matrices, namely, $\boldsymbol{S}_i^x$, $\boldsymbol{S}_i^y$ and $\boldsymbol{S}_i^z$, are introduced as

$$\boldsymbol{S}_i^x \equiv \begin{bmatrix} s_{i,1}^x \cdots s_{i,m_i}^x \\ 0 \cdots 0 \\ 0 \cdots 0 \end{bmatrix}; \boldsymbol{S}_i^y \equiv \begin{bmatrix} 0 \cdots 0 \\ s_{i,1}^y \cdots s_{i,m_i}^y \\ 0 \cdots 0 \end{bmatrix}; \text{and } \boldsymbol{S}_i^z \equiv \begin{bmatrix} 0 \cdots 0 \\ 0 \cdots 0 \\ s_{i,1}^z \cdots s_{i,m_i}^z \end{bmatrix} \tag{2a}$$

where $s_{i,1}^x \cdots s_{i,m_i}^x$ denote the shape functions along $\hat{X}_{i+1}$ axis corresponding to the m_i modes. Similarly, $s_{i,1}^y \cdots s_{i,m_i}^y$ and $s_{i,1}^z \cdots s_{i,m_i}^z$ represent the shape functions of the link along $\hat{Y}_{i+1}$ and $\hat{Z}_{i+1}$ axes in m_i modes, respectively. The overall shape function matrix of the i^{th} flexible beam vibrating in m_i modes is thus given by

$$\boldsymbol{S}_i \equiv \begin{bmatrix} \boldsymbol{S}_i^x & \boldsymbol{S}_i^y & \boldsymbol{S}_i^z \end{bmatrix} \tag{2b}$$

Moreover, three m_i-dimensional vectors, $\boldsymbol{d}_i^x$, $\boldsymbol{d}_i^y$ and $\boldsymbol{d}_i^z$, are introduced as

$$\boldsymbol{d}_i^x \equiv \begin{bmatrix} d_{i,1}^x \cdots d_{i,m_i}^x \end{bmatrix}^T; \boldsymbol{d}_i^y \equiv \begin{bmatrix} d_{i,1}^y \cdots d_{i,m_i}^y \end{bmatrix}^T \text{and } \boldsymbol{d}_i^z \equiv \begin{bmatrix} d_{i,1}^z \cdots d_{i,m_i}^z \end{bmatrix}^T \tag{2c}$$

where the vectors, $\boldsymbol{d}_i^x$, $\boldsymbol{d}_i^y$ and $\boldsymbol{d}_i^z$, are respectively the vectors of time dependent amplitudes corresponding to the shape function along $\hat{X}_{i+1}$, $\hat{Y}_{i+1}$ and $\hat{Z}_{i+1}$ axes, eq. (2a). The components of $\boldsymbol{d}_i^x$, $\boldsymbol{d}_i^y$ and $\boldsymbol{d}_i^z$, are treated here as the generalized coordinates to describe the deflection of the i^{th} link, along with those associated with the joint displacement of the i^{th} joint, namely, θ_i. Next, the $3m_i$-dimensional vector of time dependent amplitudes, $\boldsymbol{d}_i$, is defined by

$$\boldsymbol{d}_i \equiv \begin{bmatrix} \begin{bmatrix} \boldsymbol{d}_i^x \end{bmatrix}^T & \begin{bmatrix} \boldsymbol{d}_i^y \end{bmatrix}^T & \begin{bmatrix} \boldsymbol{d}_i^z \end{bmatrix}^T \end{bmatrix}^T \tag{2d}$$

Combining eqs. (2b-d), eq. (1c) is expressed as

$$\boldsymbol{u}_i = \boldsymbol{S}_i \boldsymbol{d}_i \tag{2e}$$

where the 3-dimensional vector, $\boldsymbol{u}_i$, is defined in eq. (1a).

3 SOME DEFINITIONS

Referring to the serial flexible robots, Figs. (1) and (2), following definitions are introduced:

- $\boldsymbol{t}_i$ and $\boldsymbol{w}_i$: The $(6+3m_i)$-dimensional twist and wrench of the i^{th} flexible link, i.e.,

$$\boldsymbol{t}_i \equiv \begin{bmatrix} \boldsymbol{v}_i^T & \boldsymbol{\omega}_i^T & \dot{\boldsymbol{d}}_i^T \end{bmatrix}^T; \boldsymbol{w}_i \equiv \begin{bmatrix} \boldsymbol{f}_i^T & \boldsymbol{n}_i^T & \boldsymbol{\varepsilon}_i^T \end{bmatrix}^T \tag{3}$$

where, $\boldsymbol{v}_i$ and $\boldsymbol{\omega}_i$, are the 3-dimensional vectors of velocity of the point, O_i, of the i^{th} link, and its angular velocity, respectively. Moreover, the $3m_i$-dimensional vector, $\dot{\boldsymbol{d}}_i$, is the time derivatives of the time dependent variables $\boldsymbol{d}_i$ defined in eqs. (2c). The 3-dimensional vectors, $\boldsymbol{f}_i$ and $\boldsymbol{n}_i$, are the force at O_i and the moment about O_i of the i^{th} link, respectively, whereas $\boldsymbol{\varepsilon}_i$ is the $3m_i$-dimensional generalized force vector associated with the generalized coordinates $\boldsymbol{d}_i$ due to bending.

- $\boldsymbol{t}$ and $\boldsymbol{w}$: The $\hat{n} \equiv (6+3m_i)n$ -dimensional vectors of generalized twist and wrench, respectively, which are defined as

$$\boldsymbol{t} \equiv \begin{bmatrix} \boldsymbol{t}_1^T & \boldsymbol{t}_2^T & \cdots & \boldsymbol{t}_n^T \end{bmatrix}^T; \boldsymbol{w} \equiv \begin{bmatrix} \boldsymbol{w}_1^T & \boldsymbol{w}_2^T & \cdots & \boldsymbol{w}_n^T \end{bmatrix}^T \tag{4}$$

where, $\boldsymbol{t}_i$ and $\boldsymbol{w}_i$, for i=1, …, n, are given by eq. (4).

- $\boldsymbol{q}_i$ and $\boldsymbol{\tau}_i$: The $(1+3m_i)$-dimensional vectors of joint-and-amplitudes, and the corresponding generalized forces of the i^{th} flexible link, i.e.,

$$\boldsymbol{q}_i \equiv \begin{bmatrix} \theta_i & \boldsymbol{d}_i^T \end{bmatrix}^T \text{and } \boldsymbol{\tau}_i \equiv \begin{bmatrix} \tau_i & \boldsymbol{\varepsilon}_i^T \end{bmatrix}^T \tag{5}$$

where θ_i is the rotational or translational displacement of the i^{th} joint depending on its type, i.e., revolute or prismatic, respectively, and vector $\boldsymbol{d}_i$ is defined in eq. (2c).
Moreover, τ_i, and the vector, $\boldsymbol{\varepsilon}_i$, are respectively the generalized forces corresponding to the joint coordinate, θ_i, and the amplitude vectors, $\boldsymbol{d}_i$.

- $\dot{\boldsymbol{q}}$ and $\boldsymbol{\tau}$: The $\bar{n}$-dimensional vector of rates of joint-and-amplitude vector, and the vector of corresponding generalized forces, i.e.,

$$\dot{\boldsymbol{q}} \equiv \begin{bmatrix} \dot{\boldsymbol{q}}_1 & \dot{\boldsymbol{q}}_2 & \cdots & \dot{\boldsymbol{q}}_n \end{bmatrix}^T \text{ and } \boldsymbol{\tau} \equiv \begin{bmatrix} \boldsymbol{\tau}_1 & \boldsymbol{\tau}_2 & \cdots & \boldsymbol{\tau}_n \end{bmatrix}^T \tag{6}$$

where $\dot{\boldsymbol{q}}_i$ is the time-rate of change of the joint-and-amplitude vector of the i^{th} flexible link, and $\boldsymbol{\tau}_i$ is the corresponding generalized forces of the i^{th} flexible link.

4 DYNAMIC MODELING

In this section, first, the derivation of the DeNOC matrices associated with the velocity constraints of the moving links in a serial-chain robotic system with flexible links is outlined.

4.1 The DeNOC matrices for flexible robots

The DeNOC matrices for serial flexible robots are derived below:
1) The twist of the i^{th} link is expressed in terms of the twist of $(i\text{-}1)^{\text{st}}$ link as

$$\boldsymbol{t}_i = \boldsymbol{A}_{i,i-1}\boldsymbol{t}_{i-1} + \boldsymbol{P}_i\dot{\boldsymbol{q}}_i \tag{7}$$

where $\boldsymbol{t}_i$ is the $(6+3m_i)$-dimensional twist vector of the i^{th} flexible link defined in eq. (3), and $\dot{\boldsymbol{q}}_i$ is the time-rate of change of vector $\boldsymbol{q}_i$ defined in eq. (5), whereas the $(6+3m_i)\times(6+3m_i)$ twist propagation matrix, $\boldsymbol{A}_{i,i\text{-}1}$, and the $(6+3m_i)\times(1+3m_i)$ joint-and-amplitude propagation matrix, $\boldsymbol{P}_i$, for the flexible links are as follows:

$$\boldsymbol{A}_{i,i-1} \equiv \begin{bmatrix} \boldsymbol{R}_{i,i-1} & \boldsymbol{F}_{i-1} \\ \widetilde{\boldsymbol{O}} & \overline{\boldsymbol{O}} \end{bmatrix};\ \boldsymbol{P}_i \equiv \begin{bmatrix} \boldsymbol{p}_i & \widetilde{\boldsymbol{O}}^T \\ \widetilde{\boldsymbol{0}} & \overline{\boldsymbol{1}} \end{bmatrix} \tag{8}$$

In eq. (8), the 6×6 matrix, $\boldsymbol{R}_{i,i-1}$, and the 6-dimensional vector, $\boldsymbol{p}_i$, are defined as,

$$\boldsymbol{R}_{i,i-1} \equiv \begin{bmatrix} \boldsymbol{1} & \boldsymbol{a}_{i,i-1}\times\boldsymbol{1} \\ \boldsymbol{O} & \boldsymbol{1} \end{bmatrix};\ \boldsymbol{p}_i \equiv \begin{bmatrix} \boldsymbol{0} \\ \boldsymbol{z}_i \end{bmatrix} \text{ for revolute; } \boldsymbol{p}_i \equiv \begin{bmatrix} \boldsymbol{z}_i \\ \boldsymbol{0} \end{bmatrix} \text{ for prismatic} \tag{9}$$

in which, $\boldsymbol{a}_{i,i-1} \equiv -\boldsymbol{a}_{i-1,i}$, is the position vector of the point, O_i, from O_{i-1}. Moreover, the 3×3 cross product tensor, $\boldsymbol{a}_{i,i\text{-}1}\times\boldsymbol{1}$, associated with the vector, $\boldsymbol{a}_{i,i\text{-}1}$ [19], is defined such that $(\boldsymbol{a}_{i,i\text{-}1}\times\boldsymbol{1})\boldsymbol{x} = \boldsymbol{a}_{i,i\text{-}1}\times\boldsymbol{x}$, for any 3-dimensional Cartesian vector $\boldsymbol{x}$. Furthermore, $\boldsymbol{z}_i$ is the 3-dimensional unit vector along the axis of rotation of a revolute joint or along the direction of a prismatic joint, whereas $\boldsymbol{O}$ and $\boldsymbol{0}$ are respectively the 3×3 zero matrix, and the 3-dimensional zero vector, and $\boldsymbol{1}$ is the 3×3 identity matrix. Furthermore, the $6\times 3m_i$ matrix, $\boldsymbol{F}_{i-1}$, is given by

$$\boldsymbol{F}_{i-1} \equiv \begin{bmatrix} \boldsymbol{S}_{i-1} \\ \boldsymbol{\Delta}_{i-1} \end{bmatrix} \tag{10}$$

Note that the $3\times 3m_i$ matrix, $\boldsymbol{S}_{i-1}$, contains the shape functions corresponding to the three dimensional bending deflections, as defined in eqs. (2a-b), whereas the $3\times 3m_i$ matrix, $\boldsymbol{\Delta}_{i-1}$, contains the first derivatives of the bending shape functions, corresponding to the $(i\text{-}1)^{\text{st}}$ flexible link. For the i^{th} flexible link, if s_{ij} denotes the shape function corresponding to the j^{th}

mode, its first derivative with respect to its length, $\bar{a}_i$, evaluated at the link end, a_i, is given by $\partial s_{ij}/\partial \bar{a}_i\big|_{a_i}$. Accordingly, the matrix $\boldsymbol{\Delta_i}$ is represented as

$$\boldsymbol{\Delta_i} \equiv \begin{bmatrix} 0\cdots 0 & 0\cdots 0 & 0\cdots 0 \\ 0\cdots 0 & 0\cdots 0 & -\dfrac{\partial s^{y}_{i,1}}{\partial \bar{a}_i}\Big|_{a_i} \cdots -\dfrac{\partial s^{y}_{i,m_i}}{\partial \bar{a}_i}\Big|_{a_i} \\ 0\cdots 0 & \dfrac{\partial s^{z}_{i,1}}{\partial \bar{a}_i}\Big|_{a_i} \cdots \dfrac{\partial s^{z}_{i,m_i}}{\partial \bar{a}_i}\Big|_{a_i} & 0\cdots 0 \end{bmatrix} \tag{11}$$

in which $s^{y}_{i,j}$ and $s^{z}_{i,j}$ for j=1,…, m_i are those appeared in eq. (2a). Note that $\widetilde{\boldsymbol{O}}$ and $\overline{\boldsymbol{O}}$ in eqs. (8-9) are respectively the $3m_i \times 6$ and $(3m_i \times 3m_i)$ zero matrices. Also, $\widetilde{\mathbf{0}}$ and $\bar{\mathbf{1}}$ are respectively the $3m_i$-dimensional vectors of zeros and the $3m_i \times 3m_i$ identity matrix. The $(6+3m_i)\times(6+3m_i)$ matrix, $\boldsymbol{A}_{i,i\text{-}1}$, is termed here as the twist propagation matrix for the flexible link which satisfies the property, $\boldsymbol{A_{i,j}A_{j,k}} = \boldsymbol{A_{i,k}}$. Similarly, the $(6+3m_i)\times(1+3m_i)$ matrix, $\boldsymbol{P}_i$, is termed as the joint-and-amplitude propagation matrix.

2) Now, for the n-link serial flexible robot, Figs. (1) and (2), the $\hat{n}$–dimensional vector of generalized twist, $\boldsymbol{t}$ of eq. (4), can be expressed using eq. (7) as

$$\boldsymbol{t} = \boldsymbol{A}\boldsymbol{t} + \boldsymbol{N}_d\dot{\boldsymbol{q}} \tag{12}$$

where $\boldsymbol{q}$ is the $\bar{n}$-dimensional vector of the joint-and-amplitude of the robot. In eq. (12), the $\hat{n}\times\hat{n}$ matrix, $\boldsymbol{A}$, and the $\hat{n}\times\bar{n}$ matrix, $\boldsymbol{N}_d$, are given by

$$\boldsymbol{A} \equiv \begin{bmatrix} \boldsymbol{O} & \cdots & \cdots & \boldsymbol{O} \\ \boldsymbol{A}_{21} & \boldsymbol{O} & \cdots & \boldsymbol{O} \\ \vdots & \vdots & \ddots & \vdots \\ \boldsymbol{O} & \cdots & \boldsymbol{A}_{n,n-1} & \boldsymbol{O} \end{bmatrix} ; \quad \boldsymbol{N_d} \equiv \begin{bmatrix} \boldsymbol{P}_1 & \mathbf{0} & \cdots & \mathbf{0} \\ \mathbf{0} & \boldsymbol{P}_2 & \cdots & \mathbf{0} \\ \vdots & \vdots & \ddots & \\ \mathbf{0} & \mathbf{0} & \cdots & \boldsymbol{P}_{\mathrm{n}} \end{bmatrix} \tag{13}$$

where $\boldsymbol{O}$ and $\mathbf{0}$ are the $(6+3m_i)\times(6+3m_i)$ matrix and the $(6+3m_i)$–dimensional vector of zeros, respectively. Henceforth, $\boldsymbol{O}$ and $\mathbf{0}$ should be understood as of compatible dimensions based on the expressions where they appear.

3) Equation (12) is rearranged and written as

$$\boldsymbol{t} = \boldsymbol{N}\dot{\boldsymbol{\theta}}, \text{ where } \boldsymbol{N} \equiv \boldsymbol{N_l}\boldsymbol{N_d} \tag{14}$$

In eq. (14), the $\hat{n}\times\hat{n}$ matrix, $\boldsymbol{N}_l$, is given by:

$$\boldsymbol{N_l} \equiv \begin{bmatrix} \mathbf{1} & \boldsymbol{O} & \cdots & \boldsymbol{O} \\ \boldsymbol{A}_{21} & \mathbf{1} & \cdots & \boldsymbol{O} \\ \vdots & \vdots & \ddots & \\ \boldsymbol{A}_{n1} & \boldsymbol{A}_{n2} & \cdots & \mathbf{1} \end{bmatrix} \tag{15}$$

where, $\mathbf{1}$ denotes the $(6+3m_i)\times(6+3m_i)$ identity matrix. Like $\boldsymbol{O}$ and $\mathbf{0}$, henceforth, $\mathbf{1}$ should be understood as of compatible size based on where it appears. The matrix, $\boldsymbol{N}$, in a coupled form is the NOC matrix for the serial flexible robot, as reported in [11], which are referred here as the decoupled natural orthogonal complement (DeNOC) matrices for flexible robots. The DeNOC matrices, allow one to write the matrix and vector elements associated with the dynamic equations of motion in analytical form leading to recursive forward dynamics algorithm.

4.2 Model for Flexible robots

The dynamic model for the flexible robot shown in Fig. (1) is now derived using the hybrid

EL-NE methodology and the DeNOC matrices derived above. The steps are outlined below:
1) Referring to Fig. (2), the position vectors of the elements, $\overline{E}_i$, $\widetilde{E}_i$ and payload of mass m_{pi}, on the i^{th} link, namely, $\boldsymbol{r}_i$, $\widetilde{\boldsymbol{r}}_i$ and $\boldsymbol{r}_{pi}$ are respectively given by,

$$\begin{aligned}
&\boldsymbol{r}_i = \boldsymbol{o}_i + \overline{\boldsymbol{b}}_i, \text{ where } \overline{\boldsymbol{b}}_i = \overline{b}_i \boldsymbol{z}_i;\\
&\widetilde{\boldsymbol{r}}_i = \boldsymbol{o}_i + \overline{\boldsymbol{r}}_i, \text{ where } \overline{\boldsymbol{r}}_i = b_i \boldsymbol{z}_i + \overline{a}_i \hat{\boldsymbol{x}}_{i+1} + \boldsymbol{u}_i, \text{ and}\\
&\boldsymbol{r}_{pi} = \boldsymbol{o}_i + \overline{\boldsymbol{r}}_{pi}, \text{ where } \overline{\boldsymbol{r}}_{pi} = b_i \boldsymbol{z}_i + a_i \hat{\boldsymbol{x}}_{i+1} + \boldsymbol{u}_{pi}
\end{aligned} \tag{16}$$

in which a_i and b_i, are the DH-parameters of the link, as defined in [19], $\overline{b}_i$ is the axial distance of element $\overline{E}_i$ along Z_i from O_i, and $\overline{a}_i$ is the axial distance of element $\widetilde{E}_i$ along $\hat{X}_{i+1}$ from O_i', as shown in Fig. (1). Note that $\overline{\boldsymbol{b}}_i$ is the position vector of element $\overline{E}_i$ along Z_i from O_i, whose magnitude is $\overline{b}_i$. Moreover, the unit vectors along Z_i and $\hat{X}_{i+1}$-axes are denoted with $\boldsymbol{z}_i$ and $\hat{\boldsymbol{x}}_{i+1}$, respectively, and vector $\boldsymbol{o}_i$ denotes the position vector of the point, O_i, of the i^{th} frame with respect to the origin of the fixed first frame. Furthermore, vectors $\boldsymbol{u}_i$ and $\boldsymbol{u}_{pi}$ are respectively the positions of the element, $\widetilde{E}_i$, and the payload m_{pi}, on the deformed flexible link from its undeformed state. Vector $\boldsymbol{u}_i$ is indicated in Fig. (2). Note that, the payload is considered as a concentrated point mass at the tip of the link that accounts for any assembly with sensors attached to the i^{th} link, and the real load to be carried out by the last link, etc.
2) The kinetic energy, T_i, for the i^{th} flexible link is then given by

$$T_i = \frac{1}{2}\int_0^{b_i} \rho_i \dot{\boldsymbol{r}}_i^T \dot{\boldsymbol{r}}_i \mathrm{d}\overline{b}_i + \frac{1}{2}\int_0^{a_i} \rho_i \dot{\widetilde{\boldsymbol{r}}}_i^T \dot{\widetilde{\boldsymbol{r}}}_i \mathrm{d}\overline{a}_i + \frac{1}{2} m_{pi} \dot{\boldsymbol{r}}_{pi}^T \dot{\boldsymbol{r}}_{pi} + T_{hi} \tag{17}$$

where ρ_i is the mass per unit length of the i^{th} link, and the vectors, $\dot{\boldsymbol{r}}_i$, $\dot{\widetilde{\boldsymbol{r}}}_i$ and $\dot{\boldsymbol{r}}_{pi}$, are the velocities of the elements, $\overline{E}_i$, $\widetilde{E}_i$ and payload, respectively, which is written from eq. (16) as

$$\dot{\boldsymbol{r}}_i = \boldsymbol{v}_i + \boldsymbol{\omega}_i \times \overline{\boldsymbol{b}}_i;\ \dot{\widetilde{\boldsymbol{r}}}_i = \boldsymbol{v}_i + \boldsymbol{\omega}_i \times \overline{\boldsymbol{r}}_i + \dot{b}_i \boldsymbol{z}_i + \dot{\boldsymbol{u}}_i;\ \text{and } \dot{\boldsymbol{r}}_{pi} = \boldsymbol{v}_i + \boldsymbol{\omega}_i \times \overline{\boldsymbol{r}}_{pi} + \dot{b}_i \boldsymbol{z}_i + \dot{\boldsymbol{u}}_{pi} \tag{18}$$

where, $\boldsymbol{v}_i$ is substituted for $\dot{\boldsymbol{o}}_i$, i.e., $\boldsymbol{v}_i \equiv \dot{\boldsymbol{o}}_i$. Moreover, $\dot{\overline{a}}_i = \dot{a}_i = 0$ is used in eq. (18) due to the assumption that no extension along $\hat{X}_{i+1}$ axis of the i^{th} flexible link shown in Fig. (2) is possible. Similarly, $\dot{\overline{b}}_i = 0$, as the link is rigid along Z_i-axis. Furthermore, $\dot{b}_i$ represents the linear joint rate in the presence of prismatic joint. Note that if the i^{th} joint is revolute then, $\dot{b}_i = 0$. Also, the term, T_{hi}, represents the kinetic energy due to the hub inertia at the joint. A hub can include the effect of a motor and the gear assembly at the joints given by

$$T_{hi} = 1/2\, \boldsymbol{\omega}_i^T \boldsymbol{I}_{hi} \boldsymbol{\omega}_i \tag{19}$$

where $\boldsymbol{I}_{hi}$ is the 3×3 inertia tensor for the hub.
3) The EL equations of motion for the whole system are then given by [7]:

$$\frac{d}{dt}\left(\frac{\partial T}{\partial \dot{\boldsymbol{q}}_i}\right) - \frac{\partial T}{\partial \boldsymbol{q}_i} = \boldsymbol{\tau}_i, \text{ for } i = 1, \cdots, n \tag{20}$$

where n is the total number of flexible links, whereas $\boldsymbol{q}_i$ is the $(1+3m_i)$ - dimensional vector of independent generalized coordinates defined in eq. (5). Accordingly, vector $\boldsymbol{\tau}_i$ is the associated generalized forces given by $\boldsymbol{\tau}_i \equiv \boldsymbol{\tau}_i^E + \boldsymbol{\tau}_i^s$, in which $\boldsymbol{\tau}_i^E$ is the generalized forces due to external forces and moments on the whole system, and $\boldsymbol{\tau}_i^s$ is the generalized forces due

to strains in the i^{th} link. Vector $\boldsymbol{\tau}_i^s$ has the following form:

$$\boldsymbol{\tau}_i^s \equiv \partial V_s / \partial \boldsymbol{q}_i \tag{20a}$$

where V_s is the potential energy of the system at hand due to strains. Note here that the effect of potential energy due to gravity is included by adding negative acceleration due to gravity to the linear acceleration of the first link, $\dot{\boldsymbol{v}}_1$, as proposed in Walker and Orin [27] Potential energy of the system at hand due to strain energy, V_s, is evaluated as:

$$V_s = \sum_{i=1}^{n_f} V_{si} \text{ , where } V_{si} \equiv \frac{1}{2}\int_0^{a_i} E_i I_i^y \left(\frac{\partial^2 u_i^y}{\partial \bar{a}_i^2}\right)^2 \mathrm{d}\bar{a}_i + \frac{1}{2}\int_0^{a_i} E_i I_i^z \left(\frac{\partial^2 u_i^z}{\partial \bar{a}_i^2}\right)^2 \mathrm{d}\bar{a}_i \tag{20b}$$

where $E_i I_i^y$ are the flexure rigidity and $E_i I_i^z$ is the torsional rigidity of the i^{th} link, in which E_i is the Young's modulus of elasticity, I_i^y and I_i^z are the moment of inertia of the link about its $\hat{Y}_{i+1}$ and $\hat{Z}_{i+1}$ axes, respectively. Now, the partial differentiation of V_s with respect to $\boldsymbol{q}_i$, as required in eq. (20a), is evaluated. Note that the vector of generalized coordinates, $\boldsymbol{q}_i$ is the array of θ_i , $\boldsymbol{d}_i^y$, $\boldsymbol{d}_i^z$ and $\boldsymbol{c}_i$, but V_s is a function of only $\boldsymbol{d}_i^y$, $\boldsymbol{d}_i^z$ and $\boldsymbol{c}_i$. As a result, $\boldsymbol{\tau}_i^s \equiv \partial V_s / \partial \boldsymbol{q}_i$ is obtained as

$$\boldsymbol{\tau}_i^s = \begin{bmatrix} 0 & \mathbf{0}^T & \left[\boldsymbol{\tau}_i^{sy}\right]^T & \left[\boldsymbol{\tau}_i^{sz}\right]^T \end{bmatrix}^T \tag{20c}$$

Since the strain energy due to axial centrifugal stiffening is neglected, the m_i-dimensional zero vector $\mathbf{0}$ appears in $\boldsymbol{\tau}_i^s$ after the scalar zero of eq. (20c). In eq. (20c), the m_i-dimensional vectors, $\boldsymbol{\tau}_i^{sy}$ and $\boldsymbol{\tau}_i^{sz}$, are given by,

$$\boldsymbol{\tau}_i^{sy} \equiv \begin{bmatrix} \tau_{i1}^{sy} & \cdots & \tau_{im_i}^{sy} \end{bmatrix}^T \text{and } \boldsymbol{\tau}_i^{sz} \equiv \begin{bmatrix} \tau_{i1}^{sz} & \cdots & \tau_{im_i}^{sz} \end{bmatrix}^T \tag{20d}$$

where τ_{ij}^{sy} and τ_{ij}^{sz}, for j=1,…, m_i, are as follows:

$$\tau_{ij}^{sy} \equiv E_i I_i^y \int_0^{a_i} \left(\tilde{k}_{ij}^y \sum_{h=1}^{m_i} \tilde{k}_{ih}^y d_{ih}^y \right) \mathrm{d}\bar{a}_i \text{ and } \tau_{ij}^{sz} \equiv E_i I_i^z \int_0^{a_i} \left(\tilde{k}_{ij}^z \sum_{h=1}^{m_i} \tilde{k}_{ih}^z d_{ih}^z \right) \mathrm{d}\bar{a}_i \tag{20e}$$

in which $\tilde{k}_{ij}^y \equiv \dfrac{\partial^2 s_{ij}^y}{\partial \bar{a}_i^2}$, and $\tilde{k}_{ij}^z \equiv \dfrac{\partial^2 s_{ij}^z}{\partial \bar{a}_i^2}$ for j=1, …, m_i —— s_{ij}^y and s_{ij}^z being the shape functions of the link in its j^{th} mode of vibration corresponding to the $\hat{Y}_{i+1}$ and $\hat{Z}_{i+1}$ axes respectively. Note that $d_{i,h}^y$, and $d_{i,h}^z$ are the generalized coordinates of the system. The total kinetic energy of the system is then, $T = \sum_{i=1}^{n} T_i - n$ being the total number of links in the systems. The dynamic equations of motion, as derived in Appendix A, are accordingly expressed as

$$\begin{bmatrix} \left(\dfrac{\partial \boldsymbol{t}_1}{\partial \dot{\boldsymbol{q}}_i}\right)^T & \cdots & \left(\dfrac{\partial \boldsymbol{t}_n}{\partial \dot{\boldsymbol{q}}_i}\right)^T \end{bmatrix} \begin{bmatrix} \boldsymbol{w}_1^* \\ \vdots \\ \boldsymbol{w}_n^* \end{bmatrix} = \boldsymbol{\tau}_i \text{, for } i = 1, \cdots, n \tag{21}$$

where the $(6+3m_i)\times(1+3m_i)$ matrix, $\partial \boldsymbol{t}_i / \partial \dot{\boldsymbol{q}}_j$, and the $(6+3m_i)$-dimensional vector, $\boldsymbol{w}_i^*$, for $i = 1, \cdots, n$, are reproduced from eq. (A.9) as

$$\frac{\partial \boldsymbol{t}_i}{\partial \dot{\boldsymbol{q}}_j} \equiv \begin{bmatrix} \dfrac{\partial \boldsymbol{v}_i}{\partial \dot{\boldsymbol{q}}_j} \\ \dfrac{\partial \boldsymbol{\omega}_i}{\partial \dot{\boldsymbol{q}}_j} \\ \dfrac{\partial \dot{\boldsymbol{d}}_i}{\partial \dot{\boldsymbol{q}}_j} \end{bmatrix}; \quad \boldsymbol{w}_i^* \equiv \begin{bmatrix} \int_0^{b_i} \rho_i \ddot{\bar{\boldsymbol{r}}}_i \mathrm{d}\bar{b}_i + \int_0^{a_i} \rho_i \ddot{\bar{\boldsymbol{r}}}_i \mathrm{d}\bar{a}_i + m_{pi} \ddot{\boldsymbol{r}}_{pi} \\ \int_0^{b_i} \rho_i \bar{b}_i (\boldsymbol{z}_i \times \ddot{\bar{\boldsymbol{r}}}_i) \mathrm{d}\bar{b}_i + \int_0^{a_i} \rho_i (\bar{\boldsymbol{r}}_i \times \ddot{\bar{\boldsymbol{r}}}_i) \mathrm{d}\bar{a}_i + m_{pi} (\bar{\boldsymbol{r}}_{pi} \times \ddot{\boldsymbol{r}}_{pi}) + (\boldsymbol{I}_{hi} \dot{\boldsymbol{\omega}}_i + \boldsymbol{\omega}_i \times \boldsymbol{I}_{hi} \boldsymbol{\omega}_i) \\ \int_0^{a_i} \rho_i \boldsymbol{S}_i^T \ddot{\bar{\boldsymbol{r}}}_i \mathrm{d}\bar{a}_i + m_{pi} \boldsymbol{S}_i\big|_{a_i}^T \ddot{\boldsymbol{r}}_{pi} \end{bmatrix} \tag{22}$$

where $\boldsymbol{S}_i\big|_{a_i}$ implies the value of the shape function $\boldsymbol{S}_i$, eq. (2b), evaluated at $\bar{a}_i = a_i$.

4) The vector, $\boldsymbol{w}_i^*$ of eq. (22), can be physically interpreted as the inertia wrench of the flexible link, and can be written as

$$\boldsymbol{w}_i^* = \boldsymbol{M}_i \dot{\boldsymbol{t}}_i + \boldsymbol{\gamma}_i \tag{23}$$

where $\boldsymbol{M}_i$ is the $(6+3m_i)\times(6+3m_i)$ mass matrix, and $\boldsymbol{\gamma}_i$ is the $(6+3m_i)$-dimensional vector obtained as:

$$\boldsymbol{M}_i \equiv \int_0^{b_i} \rho_i \begin{bmatrix} \boldsymbol{1} & -\bar{\boldsymbol{b}}_i \times \boldsymbol{1} & \boldsymbol{O} \\ & -\bar{\boldsymbol{b}}_i \times (\bar{\boldsymbol{b}}_i \times \boldsymbol{1}) & \boldsymbol{O} \\ sym & & \boldsymbol{O} \end{bmatrix} \mathrm{d}\bar{b}_i + \int_0^{a_i} \rho_i \begin{bmatrix} \boldsymbol{1} & -\bar{\boldsymbol{r}}_i \times \boldsymbol{1} & \boldsymbol{S}_i \\ & -\bar{\boldsymbol{r}}_i \times (\bar{\boldsymbol{r}}_i \times \boldsymbol{1}) & \bar{\boldsymbol{r}}_i \times \boldsymbol{S}_i \\ sym & & \boldsymbol{S}_i^T \boldsymbol{S}_i \end{bmatrix} \mathrm{d}\bar{a}_i + m_{pi} \begin{bmatrix} \boldsymbol{1} & -\bar{\boldsymbol{r}}_{pi} \times \boldsymbol{1} & \boldsymbol{S}_i\big|_{a_i} \\ & -\bar{\boldsymbol{r}}_{pi} \times (\bar{\boldsymbol{r}}_{pi} \times \boldsymbol{1}) & \bar{\boldsymbol{r}}_{pi} \times \boldsymbol{S}_i\big|_{a_i} \\ sym & & \boldsymbol{S}_i\big|_{ai}^T \boldsymbol{S}_i\big|_{a_i} \end{bmatrix} + \begin{bmatrix} \boldsymbol{O} & \boldsymbol{O} & \boldsymbol{O} \\ & \boldsymbol{I}_{hi} & \boldsymbol{O} \\ & & \boldsymbol{O} \end{bmatrix} \tag{24a}$$

$$\gamma_i \equiv \int_0^{b_i} \rho_i \begin{bmatrix} \bar{\boldsymbol{\varpi}}_i \\ \bar{\boldsymbol{b}}_i \times \bar{\boldsymbol{\varpi}}_i \\ \boldsymbol{0} \end{bmatrix} \mathrm{d}\bar{b}_i + \int_0^{a_i} \rho_i \begin{bmatrix} \boldsymbol{\varpi}_i \\ \bar{\boldsymbol{r}}_i \times \boldsymbol{\varpi}_i \\ S_i^T \boldsymbol{\varpi}_i \end{bmatrix} \mathrm{d}\bar{a}_i + m_{pi} \begin{bmatrix} \boldsymbol{\varpi}_{pi} \\ \bar{\boldsymbol{r}}_{pi} \times \boldsymbol{\varpi}_{pi} \\ S_i\big|_{ai}^T \boldsymbol{\varpi}_{pi} \end{bmatrix} + \begin{bmatrix} \boldsymbol{0} \\ \boldsymbol{\omega}_i \times \boldsymbol{I}_{hi} \boldsymbol{\omega}_i \\ \boldsymbol{0} \end{bmatrix} \tag{24b}$$

where $\bar{\boldsymbol{\varpi}}_i \equiv \boldsymbol{\omega}_i \times (\boldsymbol{\omega}_i \times \bar{\boldsymbol{b}}_i)$, $\boldsymbol{\varpi}_i \equiv \boldsymbol{\omega}_i \times [(\boldsymbol{\omega}_i \times \bar{\boldsymbol{r}}_i) + \dot{\boldsymbol{u}}_i]$, $\boldsymbol{\varpi}_{pi} \equiv \boldsymbol{\omega}_i \times [(\boldsymbol{\omega}_i \times \bar{\boldsymbol{r}}_{pi}) + \dot{\boldsymbol{u}}_{pi}]$ and the word "*sym*" denotes the symmetric elements of the matrix, $\boldsymbol{M}_i$.

5) Combining eq.(23) for all n-links, i.e., i=1,…, n, eq.(21) can be written as

$$(\partial \boldsymbol{t}/\partial \dot{\boldsymbol{q}})^T (\boldsymbol{M}\dot{\boldsymbol{t}} + \boldsymbol{\gamma}) = \boldsymbol{\tau} \tag{25}$$

where the $\hat{n}\times\hat{n}$ matrix, $\boldsymbol{M}$, the $\hat{n}$–dimensional vector, $\boldsymbol{\gamma}$, and the $\bar{n}$–dimensional vector, $\boldsymbol{\tau}$, are given by

$$\boldsymbol{M} \equiv diag[\boldsymbol{M}_1 \quad \cdots \quad \boldsymbol{M}_n]; \; \boldsymbol{\gamma} \equiv [\boldsymbol{\gamma}_1^T \quad \cdots \quad \boldsymbol{\gamma}_n^T]^T; \text{ and } \boldsymbol{\tau} \equiv [\boldsymbol{\tau}_1 \quad \cdots \quad \boldsymbol{\tau}_n]^T \tag{26}$$

The vectors, $\boldsymbol{t}$ and $\boldsymbol{w}$, are defined in eq. (5), and the $\hat{n}\times\hat{n}$ matrix, $\partial \boldsymbol{t}/\partial \dot{\boldsymbol{q}}$, is now defined as

$$\frac{\partial \boldsymbol{t}}{\partial \dot{\boldsymbol{q}}} \equiv \begin{bmatrix} \dfrac{\partial \boldsymbol{t}_1}{\partial \dot{\boldsymbol{q}}_1} & \cdots & \dfrac{\partial \boldsymbol{t}_1}{\partial \dot{\boldsymbol{q}}_n} \\ \vdots & & \vdots \\ \dfrac{\partial \boldsymbol{t}_n}{\partial \dot{\boldsymbol{q}}_1} & \cdots & \dfrac{\partial \boldsymbol{t}_n}{\partial \dot{\boldsymbol{q}}_n} \end{bmatrix} \tag{27}$$

6) From eq. (14), it is clear that

$$\frac{\partial \boldsymbol{t}}{\partial \dot{\boldsymbol{q}}} = \boldsymbol{N}_l \boldsymbol{N}_d \tag{28}$$

Hence, eq. (25) yields

$$\boldsymbol{N}_d^T \boldsymbol{N}_l^T (\boldsymbol{M}\dot{\boldsymbol{t}} + \boldsymbol{\gamma}) = \boldsymbol{\tau} \tag{29}$$

7) Now, differentiating eq. (5) with respect to time, one obtains

$$\dot{\boldsymbol{t}} = \boldsymbol{N}_l \boldsymbol{N}_d \ddot{\boldsymbol{q}} + \boldsymbol{N}_l \dot{\boldsymbol{N}}_d \dot{\boldsymbol{q}} + \dot{\boldsymbol{N}}_l \boldsymbol{N}_d \dot{\boldsymbol{q}} \tag{30}$$

Substituting eq. (30) into eq. (29) the independent set of constraint dynamic equations of

motion for the robot with all flexible links is then obtained as

$$\boldsymbol{I}\ddot{\boldsymbol{q}} = \boldsymbol{\phi} \tag{31}$$

where $\boldsymbol{I}$ is the $\overline{n} \times \overline{n}$ Generalized Inertia Matrix (GIM) of the system. Moreover, the (i,j) element of the matrix, $\boldsymbol{I}$, are the $(1+3m_i)\times(1+3m_i)$ block matrices, which are expressed analytically by

$$\boldsymbol{I}_{ij} = \boldsymbol{I}_{ji}^{T} = \boldsymbol{P}_{\boldsymbol{i}}^{\boldsymbol{T}} \widetilde{\boldsymbol{M}}_{i} \boldsymbol{A}_{ij} \boldsymbol{P}_{\boldsymbol{j}}, \text{ for } i = 1, \ldots, n;\ j = 1, \ldots, i. \tag{32}$$

where the $(1+3m_i)\times(1+3m_i)$ matrix, $\widetilde{\boldsymbol{M}}_{\boldsymbol{i}}$, is obtained recursively, namely,

$$\widetilde{\boldsymbol{M}}_{i} \equiv \boldsymbol{M}_{i} + \boldsymbol{A}_{i+1,i}^{T} \widetilde{\boldsymbol{M}}_{i+1} \boldsymbol{A}_{i,i+1}$$

in which $\widetilde{\boldsymbol{M}}_{\boldsymbol{n}+1} \equiv \boldsymbol{O}$, as there is no $(n+1)^{\text{st}}$ link in the chain. Hence, $\widetilde{\boldsymbol{M}}_{n} \equiv \boldsymbol{M}_{n}$. Moreover, the $\overline{n}$ –dimensional vector, $\boldsymbol{\phi}$, containing the external, strain energy, Coriolis, and other velocity dependent terms is expressed as

$$\boldsymbol{\phi} = \boldsymbol{\tau} - \boldsymbol{N}_{\boldsymbol{d}}^{\boldsymbol{T}} \boldsymbol{N}_{\boldsymbol{l}}^{\boldsymbol{T}} \left[\boldsymbol{M} (\boldsymbol{N}_{l} \dot{\boldsymbol{N}}_{d} + \dot{\boldsymbol{N}}_{l} \boldsymbol{N}_{d}) \dot{\boldsymbol{q}} \right] \tag{33}$$

Equations (31)-(33) represent the analytical and recursive expressions for the matrix elements of the GIM. Similar to the rigid body system, [19], $\widetilde{\boldsymbol{M}}_{i}$ is interpreted here as the mass matrix for the "composite flexible body" comprising of the rigidly attached flexible bodies, #i, …, #n.

5 FORWARD DYNAMICS ALGORITHM

In this Section, a recursive, computationally efficient, and numerically stable algorithm for calculating the joint accelerations, $\ddot{\boldsymbol{q}}$ from eq. (31), are outlined. The GIM, $\boldsymbol{I}$ of eq. (31), is decomposed using the reverse Gaussian elimination (RGE) [15], namely,

$$\boldsymbol{I} = \boldsymbol{U}\boldsymbol{D}\boldsymbol{U}^{\boldsymbol{T}} \tag{34}$$

where $\boldsymbol{U}$ and $\boldsymbol{D}$ are respectively the $\overline{n} \times \overline{n}$ upper block triangular and block diagonal matrices, and $\overline{n}$ is the DOF of the system given by, $\overline{n} \equiv (1+3m_i)n$. Matrices $\boldsymbol{U}$ and $\boldsymbol{D}$ are given by

$$\boldsymbol{U} \equiv \begin{bmatrix} \boldsymbol{1} & \boldsymbol{U}_{12} & \cdots & \boldsymbol{U}_{1n} \\ \boldsymbol{O} & \boldsymbol{1} & \cdots & \boldsymbol{U}_{2n} \\ \vdots & \vdots & \ddots & \vdots \\ \boldsymbol{O} & \boldsymbol{O} & \cdots & \boldsymbol{1} \end{bmatrix};\ \boldsymbol{D} \equiv \begin{bmatrix} \hat{\boldsymbol{I}}_{1} & \boldsymbol{O} & \cdots & \boldsymbol{O} \\ \boldsymbol{O} & \hat{\boldsymbol{I}}_{2} & \cdots & \boldsymbol{O} \\ \vdots & \vdots & \ddots & \vdots \\ \boldsymbol{O} & \cdots & \cdots & \hat{\boldsymbol{I}}_{n} \end{bmatrix} \tag{35}$$

in which the $(1+3m_i)\times(1+3m_i)$ matrices, $\boldsymbol{U}_{\boldsymbol{ij}}$ and $\hat{\boldsymbol{I}}_{i}$, for i,j=1, …, n, are obtained from the application of the RGE rules. The expressions for $\boldsymbol{U}_{ij}$ and $\hat{\boldsymbol{I}}_{i}$ for i=1,…, n; j=i+1, …, n, are

$$\boldsymbol{U}_{ij} \equiv \boldsymbol{P}_{\boldsymbol{i}}^{\boldsymbol{T}} \boldsymbol{\Psi}_{ij}, \text{ and } \hat{\boldsymbol{I}}_{i} \equiv \boldsymbol{P}_{\boldsymbol{i}}^{\boldsymbol{T}} \hat{\boldsymbol{\Psi}}_{\boldsymbol{i}} \tag{36}$$

where $\boldsymbol{P}_{i}$ is the $(6+3m_i)\times(1+3m_i)$ -dimensional joint-and-amplitude propagation matrix, as defined in eq. (8), and the $(6+3m_i)\times(1+3m_i)$ matrices, $\hat{\boldsymbol{\Psi}}_{\boldsymbol{i}}$ and $\boldsymbol{\Psi}_{ij}$ are given by

$$\hat{\boldsymbol{\Psi}}_{\boldsymbol{i}} \equiv \hat{\boldsymbol{M}}_{\boldsymbol{i}} \boldsymbol{P}_{\boldsymbol{i}};\ \boldsymbol{\Psi}_{\boldsymbol{i}} \equiv \hat{\boldsymbol{\Psi}}_{\boldsymbol{i}} \hat{\boldsymbol{I}}_{\boldsymbol{i}}^{-1};\ \boldsymbol{\Psi}_{\boldsymbol{ij}} \equiv \boldsymbol{A}_{\boldsymbol{ji}}^{\boldsymbol{T}} \boldsymbol{\Psi}_{\boldsymbol{i}}. \tag{37}$$

Note that the matrix, $\hat{\boldsymbol{M}}_{\boldsymbol{i}}$, represents the mass and inertia properties of the articulated flexible body i, defined similar to the articulated inertia matrix for the rigid body system consisting of flexible links, #i, …, #n, which are coupled by the joints, i+1, …, n. The $(6+3m_i)\times(6+3m_i)$ matrix, $\hat{\boldsymbol{M}}_{\boldsymbol{i}}$, is obtained recursively as

$$\hat{\boldsymbol{M}}_{\boldsymbol{i}} \equiv \boldsymbol{M}_{\boldsymbol{i}} + \boldsymbol{A}_{\boldsymbol{i},\boldsymbol{i}+1}^{\boldsymbol{T}} \overline{\boldsymbol{M}}_{\boldsymbol{i}+1} \boldsymbol{A}_{\boldsymbol{i},\boldsymbol{i}+1}, \text{ where } \overline{\boldsymbol{M}}_{\boldsymbol{i}} \equiv \hat{\boldsymbol{M}}_{\boldsymbol{i}} - \hat{\boldsymbol{\Psi}}_{\boldsymbol{i}} \boldsymbol{\Psi}_{\boldsymbol{i}}^{\boldsymbol{T}} \tag{38}$$

for i=n-1, …, 1, and $\hat{\boldsymbol{M}}_{\boldsymbol{n}} \equiv \boldsymbol{M}_{\boldsymbol{n}}$. For the recursive algorithm, the $\overline{n}$ –dimensional vector of the generalized forces due to external moments, forces, gravity, strain associated with the link

deformations, and the centrifugal and Coriolis accelerations, etc., $\boldsymbol{\phi}$ of eqs. (31) and (33), are assumed to be evaluated recursively. The solution for $\ddot{\boldsymbol{q}}$ can now be obtained from eq. (31) using the following three steps:

Step A. Solution for $\hat{\boldsymbol{\phi}}$: The solution, $\hat{\boldsymbol{\phi}} = \boldsymbol{U}^{-1}\boldsymbol{\phi}$, is evaluated for, i=n-1, …,1, as

$$\hat{\boldsymbol{\phi}}_i = \boldsymbol{\phi}_i - \boldsymbol{P}_i^T \boldsymbol{\eta}_i \tag{39}$$

where $\hat{\boldsymbol{\phi}}_n \equiv \boldsymbol{\phi}_n$. Note that the (6+3$m_i$)–dimensional vector, $\boldsymbol{\eta}_i$, is obtained as

$$\boldsymbol{\eta}_i = \boldsymbol{\Psi}_i \hat{\boldsymbol{\phi}}_i + \overline{\boldsymbol{\eta}}_i;\ \overline{\boldsymbol{\eta}}_i \equiv \boldsymbol{A}_{i+1,i}^T \boldsymbol{\eta}_{i+1}, \text{ and } \overline{\boldsymbol{\eta}}_n = \boldsymbol{0}$$

Step B. Solution for $\tilde{\boldsymbol{\phi}}$: $\boldsymbol{D}\tilde{\boldsymbol{\phi}} = \hat{\boldsymbol{\phi}}$, for i= 1, …, n,

$$\tilde{\boldsymbol{\phi}}_i = \hat{\boldsymbol{I}}_i^{-1} \boldsymbol{\phi}_i \tag{40}$$

in which the (1+3m_i)×(1+3m_i) matrix, $\hat{\boldsymbol{I}}_i$, is defined in eq. (36).

Step C. Solution for $\ddot{\boldsymbol{q}}_i$: $\ddot{\boldsymbol{q}}_i \equiv \boldsymbol{U}^{-T}\tilde{\boldsymbol{\phi}}$, for i=2, …, n,

$$\ddot{\boldsymbol{q}}_i = \tilde{\boldsymbol{\phi}}_i - \boldsymbol{\Psi}_i^T \overline{\boldsymbol{\mu}}_i \tag{41}$$

where the (1+3m_i)-dimensional vector, $\ddot{\boldsymbol{q}}_1 \equiv \tilde{\boldsymbol{\phi}}_1$, and the (6+3$m_i$)-dimensional vector, $\overline{\boldsymbol{\mu}}_i$, is obtained from

$$\overline{\boldsymbol{\mu}}_i \equiv \boldsymbol{A}_{i,i-1}\boldsymbol{\mu}_{i-1} \text{ and } \boldsymbol{\mu}_i \equiv \boldsymbol{P}_i \ddot{\boldsymbol{q}}_i + \overline{\boldsymbol{\mu}}_i;\ \overline{\boldsymbol{\mu}}_1 = \boldsymbol{0} \tag{42}$$

6 COMPUTATIONAL COMPLEXITY

The computational complexity of the proposed algorithm is shown in Table 1, where it is also compared with other two algorithms, namely, [11, 29]. No other recent literature reported such complexity count except for the RR–R stands for the revolute joints─ and RRR robots [6] where only the computational complexity of the generalized inertia matrix (GIM) is reported, but not the forward dynamics algorithm. From Table 1, it is clear that the recursive algorithm proposed in this paper outperforms the other two.

Table 1 Comparison of computational complexity considering vibrations in bending ($m = 2$) only

Algorithm	**Multiplications (M)**	**Additions (A)**	n^*=8	
			M	**A**
Proposed	$M_{1p}n + M_{2p}$	$A_{1p}n + A_{2p}$	**9874**	**7699**
Jain and Rodriguez [29]	$M_{1j}n$	$A_{1j}n$	10568	8344
Cyril [11]	$M_{1c}n^3 + M_{2c}n^2 + M_{3c}n + M_{4c}$	$A_{1c}n^3 + A_{2c}n^2 + A_{3c}n + A_{4c}$	13990	12683

n^*: Number of links for which the proposed algorithm benefits over the other two algorithms

The coefficients in Table 1are:

$M_{1p} \equiv 2m^2 + 180m + 299 + M_{m3}$; $M_{2p} \equiv -(124m + 229 + M_{m4})$; $A_{1p} \equiv 6m^2 + 122m + 220 + A_{m3}$;

$A_{2p} \equiv -(94m + 192 + A_{m4})$; where

$$M_{m3} \equiv \frac{\hat{m}^3}{6} + \left(2m + \frac{15}{2}\right)\hat{m}^2 + \left(2m^2 + 15m + \frac{100}{3}\right)\hat{m};\ M_{m4} \equiv \left(2m^2 + 13m + 27\right)\hat{m};$$

$$A_{m3} \equiv \frac{\hat{m}^3}{6} + \frac{\hat{m}^2}{2} + \left(6m^2 + 27m + \frac{82}{3}\right)\hat{m};\ A_{m4} \equiv \left(2m^2 + 13m + 27\right)\hat{m}$$

$$M_{1c} \equiv \frac{\hat{m}^3}{6} + \hat{m}^2\left(-\frac{m}{2}+1\right) + \hat{m}\left(\frac{m^2}{2}-2m\right) - \frac{m^3}{6} + m^2;\ M_{2c} \equiv -\frac{3\hat{m}^2}{2} + \hat{m}\left(3m+\frac{33}{2}\right) - \frac{3m^2}{2} - \frac{15m}{2} + 12;$$

$$M_{3c} \equiv 5\hat{m}^2 - \hat{m}\left(10m+\frac{109}{6}\right) + \frac{m^3}{6} + \frac{53m^2}{6} + \frac{233m}{3} + 246;\ M_{4c} \equiv -123$$

$$A_{1c} \equiv \frac{\hat{m}^3}{6} + \hat{m}^2\left(-\frac{m}{2}+1\right) + \hat{m}\left(\frac{m^2}{2}-2m\right) - \frac{m^3}{6} + m^2;\ A_{2c} \equiv -\frac{3\hat{m}^2}{2} + \hat{m}(3m+13) - \frac{3m^2}{2} - \frac{17m}{2} + 9;$$

$$A_{3c} \equiv 5\hat{m}^2 - \hat{m}\left(10m+\frac{85}{6}\right) + \frac{m^3}{6} + \frac{53m^2}{6} - \frac{251m}{6} + 228;\ A_{4c} \equiv -102$$

$$M_{1j} \equiv \begin{cases} \dfrac{5m^3}{6} + \dfrac{27m^2}{2} + \dfrac{893m}{3} + 281 \ ; \text{for } n \le 7 \\ 13m^2 + 298m + 673 \ ; \text{for } n \ge 7 \end{cases} \quad ; \quad A_{1j} \equiv \begin{cases} \dfrac{5m^3}{6} + \dfrac{23m^2}{2} + \dfrac{677m}{3} + 256 \ ; \text{for } n \le 7 \\ 14m^2 + 225m + 537 \ ; \text{for } n \ge 7 \end{cases}$$

in which $\hat{m} = 1 + 2m$

7 SIMULATIONS

In this section, the proposed forward dynamics algorithm presented in Section 5 is validated by comparing its simulation results with those available in the literature. Numerical stability of the simulation results based on the proposed algorithm are also analyzed.

7.1 Simulation results

A 3-link Canadarm [11], with all links flexible, as shown in Fig. (3), is considered here. The DH parameters and the mass properties of the Canadarm are shown in Table 2. The data are taken from [8, 11] where detailed results are available for comparison purposes. All the flexible links are assumed to be vibrating in first two modes only since the consideration of more than first two modes do not have significant effect on the results [11-12]. The eigen function used to represent the deflection of the i^{th} link in its j^{th} mode is given by [11]:

$$s_{ij} = \left[(\sin\varsigma_j + \sinh\varsigma_j) - \sigma(\cos\varsigma_j + \cosh\varsigma_j)\right] \ ; \ \sigma = (\sin\tilde{m}_j + \sinh\tilde{m}_j)/(\cos\tilde{m}_j + \cosh\tilde{m}_j) \qquad (43)$$

Forced simulation of the robot is performed where the input joint torques, i.e., vector $\boldsymbol{\tau}$ of eq.(25), are calculated from an inverse dynamics algorithm of all rigid link Canadarm that was developed separately for the purpose. The trajectory of each revolute joint is taken as:

$$\theta_i = k_i\left[t - \frac{T_i}{\pi}\sin\left(\frac{\pi}{T_i}t\right)\right] \text{; for i=1, 2, 3} \qquad (44)$$

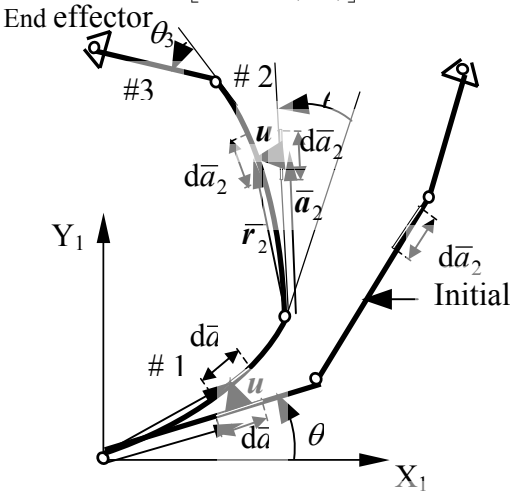

Figure 3: A 3-link Canadarm robot with all flexible links

Table 2 DH and other parameters of the Canadarm robot

Link	a_i (m)	b_i (m)	α_i (rad)	θ_i (rad)	m_i (Kg)	E_iI_i (Nm^2)
1	6	0	0	$\theta_1[0]^*$	140	1×10^5
2	7	0	0	$\theta_2[0]$	85	1×10^5
3	2	0	0	$\theta_3[0]$	95	1×10^5

* The values in [and] show the initial configuration of the arm

In eq.(44), k_1=0.075sec^{-1}, k_2=0.05sec^{-1}, k_3=0.1sec^{-1} and T_1=10sec, T_2=T_3=5sec. Figures (4-5) show the forced simulation results, where the simulated joint angles are compared with the desired trajectory that are obtained from eq. (42). The deviation of the simulated trajectories from the desired trajectory is due to the flexibility of the links. The results exactly match with those reported in [11].

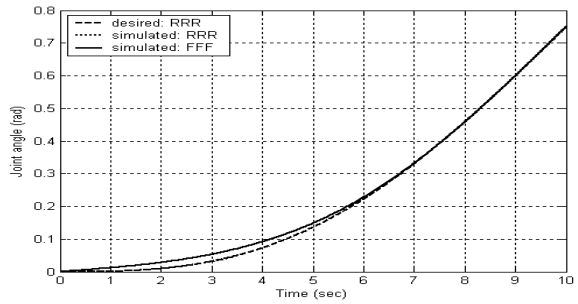

(a) Angular displacement of joint 1

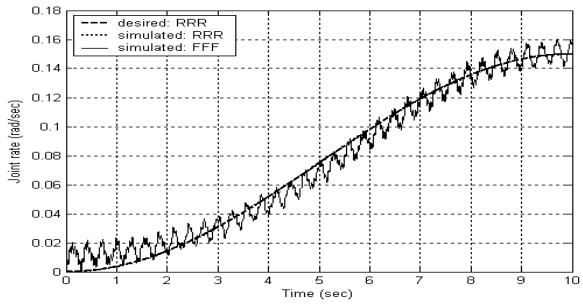

(d) Rate of angular displacement of joint 1

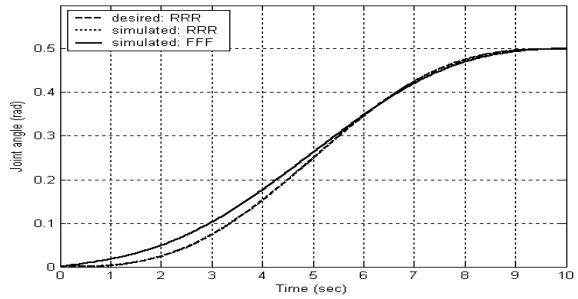

(b) Angular displacement of joint 2

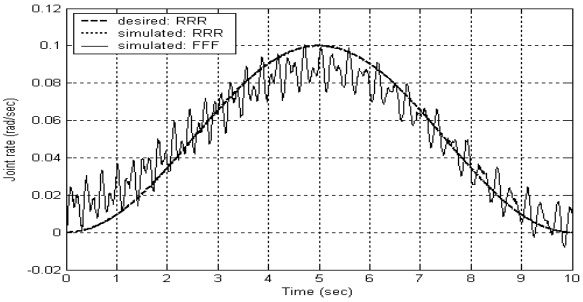

(e) Rate of angular displacement of joint 2

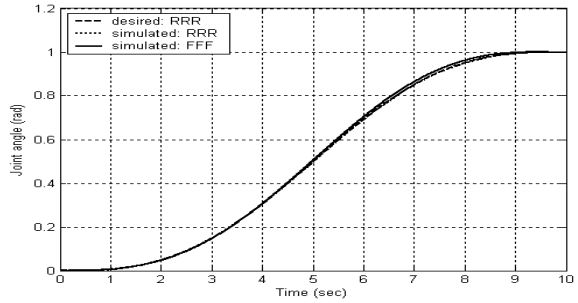

(c) Angular displacement of joint 3

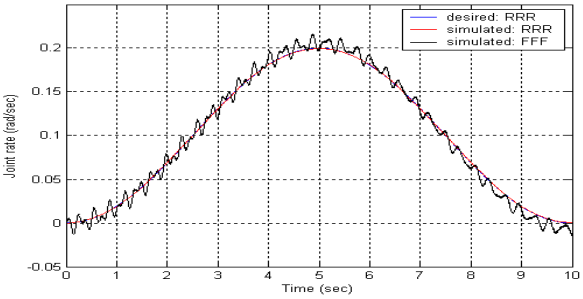

(f) Rate of angular displacement of joint 3

Figure 4: Forced simulation results for 3-link Canadarm with all links flexible

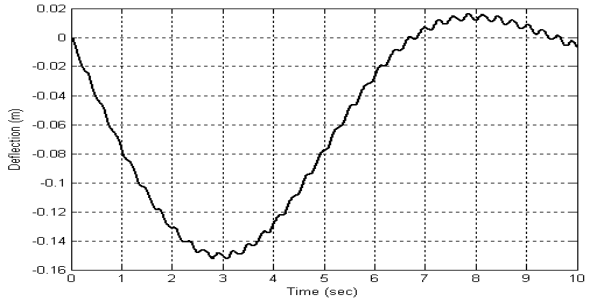

(a) Link 1

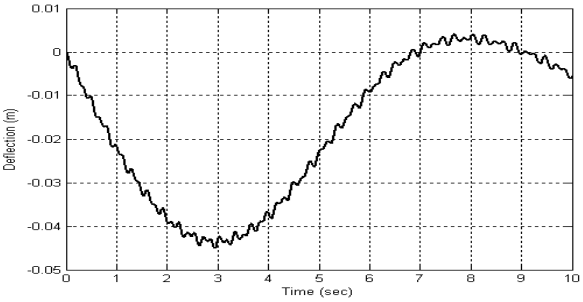

(b) Link 2

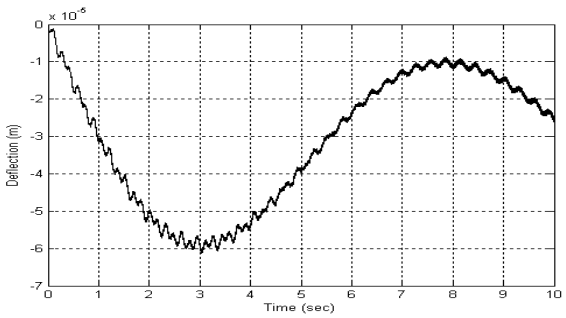

(c) Link 3

Figure 5: Tip deflection of the links of Canadarm

7.2 Numerical Stability

The numerical stability of the proposed algorithm is studied here taking the example of Canadarm. The simulation results obtained using the proposed algorithm are compared with those obtained using a non-recursive algorithm while all other calculation steps are kept same. In the non-recursive algorithm, the GIM, $\boldsymbol{I}$ of eq. (31), is first obtained numerically before it is factorized numerically using the Cholesky decomposition [15], followed by the solution of the joint accelerations, $\ddot{\boldsymbol{q}}$, using forward and backward substitutions. The algorithm is known to have $O(n^3)$ complexities [15]. The calculation of $\boldsymbol{\phi}$ is carried out exactly in a manner done for the proposed recursive algorithm. Hence, the effect of recursive and non-recursive algorithms becomes explicit. The simulation results obtained using the two algorithms are compared with the desired trajectory of eq. (44). The difference between the simulated joint path obtained from the two forward dynamics (FD) algorithms and the desired joint maneuver are plotted in Fig. (6). Results for only joint 1 are shown, as similar results are obtained for other two joints. Note that, in Fig. (6), the differences in simulation results from the desired trajectory is due to the fact that the input torques to the FD algorithms of the flexible system are calculated for the rigid-link systems. Hence, there are obvious variations in the joint angles. However, the non-recursive algorithm fails to provide any result after about 5 sec because the errors blow up and results become unstable. The results from the proposed algorithm, on the other hand, continue to give acceptable results. Hence, the proposed algorithm can be considered numerically more stable.

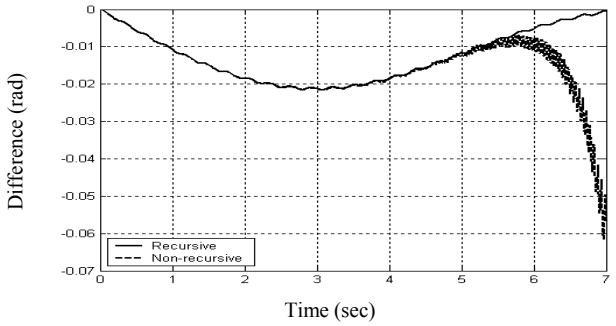

Figure 6: Comparison of simulation results for joint 1

Next, the power difference (PD) for the 3-link Canadarm is investigated for the two FD algorithms. Since a flexible link is energy dissipating system, assuming no losses due to friction and damping, the output energy is equal to the input energy supplied to the system minus the energy dissipated in vibrations. Accordingly, the output power of the system is

calculated as, $\widetilde{E}_n = \sum_{i=1}^{n} \tau_i \dot{\tilde{q}}_i$, where τ_i and $\dot{\tilde{q}}_i$ are the torque input from the inverse dynamics algorithm and the simulated joint rates, respectively, and *n* is the number of joints. The output power is calculated from both the proposed and conventional algorithms. The results are plotted in Figs. 7 (a-b). The PD for the non-recursive algorithm seems to be increasing to an unacceptable level after about 3.5sec, whereas the proposed recursive algorithm continues to provide acceptable PD, even after 7 sec. This shows that the proposed algorithm is more stable.

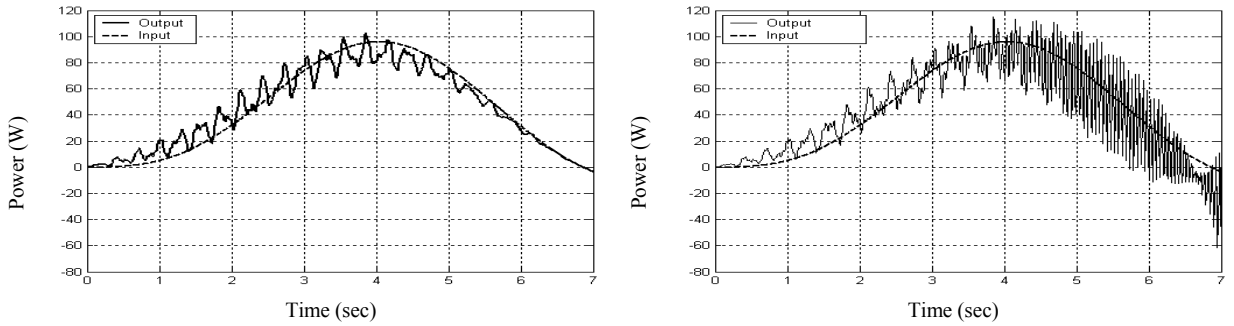

(a) Recursive (proposed) (b) Non-recursive

Figure 7: Comparison of desired and simulated powers for Canadarm using two algorithms

To further investigate the built-up of the errors, the nature of the joint accelerations, $\ddot{\theta}_i$, for *i*=1,2,3, is obtained using both the FD algorithms. As shown in Figs. 8(a-b) for joint 1, the joint acceleration curve, $\ddot{\theta}_1$, for the proposed recursive algorithm, is smoother for a longer duration of time while the same from the non-recursive algorithm is not, which shows sharp peaks after 3.5 sec. Similar behaviors are observed for $\ddot{\theta}_2$ and $\ddot{\theta}_3$ also. From the error plots and study of numerical stability from other aspects, it is concluded that the proposed FD algorithm, as given in Section 5, is numerically more stable.

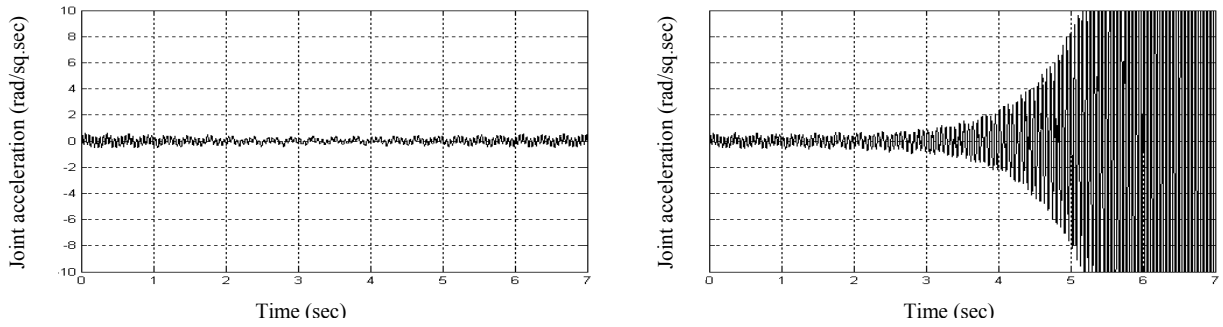

(a) Recursive (proposed) (b) Non-recursive

Figure 8: Joint accelerations at joint 1

8 CONCLUSIONS

A recursive forward dynamics algorithm for flexible link robots, based on the hybrid EL-NE equations of motion and the DeNOC matrices, is presented. The proposed forward dynamics algorithm is recursive, computationally efficient and numerically stable. One of the contributions of this paper is the stability and efficiency study and the establishment of such simulation algorithm allowing realistic and real-time simulation for the serial robotic system with all links flexible. The other contributions of this paper are: 1) simplification of the dynamic algorithm based on the assumption of link shapes as bent slender beams, which is

realistic in most practical robots; 2) Evaluation and comparison of the computational complexity of the proposed algorithm with those available in literature; 3) Simulation results for Canadarm robot considering all links flexible; 4) Stability analysis for above Canadarm; 5) Physical interpretations of many terms associated with the dynamic model of the flexible link robot systems. In future publications, the extension of the algorithm to the systems having some links rigid and some links flexible will be presented.

REFERENCES

[1] Shabana, A. A., 1997, "Flexible multibody dynamics: Review of past and recent developments," Multibody System Dynamics, 1, 189-222.
[2] Wasfy, T. M., and Noor, A. K., 2003, "Computational strategies for flexible multibody systems," ASME, J. of App. Mech. Reviews, 56 (6), 553-613.
[3] Silver, W. M., 1982, "On equivalence of Lagrangian and Newton-Euler dynamics for manipulator," Int. J. of Robotics Research, 1 (2), 60-70.
[4] Yoshikawa, T., and Hosoda, K.,1996, "Modeling of Flexible Manipulators using Virtual Rigid Links and Passive Joints," Int. J. of Robotics Research, 15 (3), 290-297.
[5] Book, W. J., 1984, "Recursive Lagrangian Dynamics of Flexible manipulator arms," Int. J. of Robotics Research, 3 (3), 87-101.
[6] Theodore, R. J., and Ghosal, A., 1995, "Comparison of the assumed modes and finite elements modes for flexible multilink manipulators," I. J. of Robotics Research, 14-2, 91-111.
[7] Shabana, A. A., 2005. *Dynamics of Multibody Systems*. Cambridge Press, Cambridge.
[8] Sharf, I., and Damaren, C., 1992, "Simulation of flexible link manipulators: basis functions and non-linear terms in motion equations," Proc. of IEEE Conf. on Robotics and Automation, France, 1956-1962.
[9] Usoro, P. B., Nadira, R., and Mahil, S. S., 1986, "A finite element/Lagrangian approach to modeling light weight flexible manipulators," ASME J. of Dyn. Sys, Meas. and Control, 108, 198-205.
[10] Chedmail, P., Aoustin, Y., and Chevallereau, Ch., 1991, "Modeling and control of flexible robots," Int. J. of Numerical Methods in Engineering, 32, 1595-1619.
[11] Cyril, X., 1988, Dynamics of flexible link manipulators, Ph.D. dissertation, McGill University, Canada.
[12] De Luca, A., and Siciliano B., 1991, "Closed-form dynamic model of planar multilink lightweight robots," IEEE Trans. on Systems, Man and Cybernetics, 21 (4), 826-838.
[13] Kim S. S., and Haug E. J., 1988, "A recursive formulation for flexible multibody dynamics, part-I: open-loop systems," Comp. methods in App. Mech. and engg., 71, 293-314.
[14] Shabana, A. A., 1990, "Dynamics of flexible bodies using generalized Newton-Euler equation," ASME J. of Dyn. Sys., Meas. and Control, 112 (3), 496-503.
[15] Strang, G., 1980. *Linear Algebra and Its Applications*. H. B. Jovanovich Pub., Florida.
[16] Saha, S. K., 1997, "A decomposition of manipulator inertia matrix," IEEE Trans. on Robotics and Automation, 13(2), 301-304.
[17] Nikravesh, P. E., 1988, *Computer-Aided Analysis of Mechanical Systems*, PH, N. Jersey.
[18] Angeles, J., and Lee, S. K., 1988, "The formulation of dynamical equations of holonomic mech. systems using a natural orthogonal complement," ASME J. of A. Mech., 55, 243-244.
[19] Saha, S. K., 1999, "Dynamic modeling of serial multi-body systems using the decoupled natural orthogonal complement matrices," ASME J. of App. Mech., 29 (2), 986-996.
[20] Saha, S. K. and Schiehlen, W. O., "Recursive kinematics and dynamics for closed loop multibody systems," Int. J. of Mech. of Struct. and Mach., 29 (2), 143-175, 2001.

[21] Khan, W. A., Krovi, V. N., Saha, S. K., and J. Angeles, "Modular and recursive kinematics and dynamics for parallel manipulators," Multibody System Dynamics, 14, 419-455, 2005.
[22] Chaudhary, H., and Saha, S. K., "Constraint force formulation for closed loop multibody systems," to appear in Tran. on ASME in Mech. Design
[23] Featherstone, R., "The calculation of robotic dynamics using articulated body inertias," Int. J. of Mechanics of structures and machines, 2 (1), 13-30, 1983.
[24] Ider, S. K., 1990, "Stability analysis of constraints in flexible multibody systems dynamics," Int. J. of Engineering Science, 28 (12), 1277-1290.
[25] Cloutier, B. P., Pai, D. K., and Ascher, U. M., 1995, "The formulation stiffness of forward dynamics algorithms and implications for robot simulation," Proc. of IEEE Conf. on Robotics and Automation, Japan, May, 2816-2822.
[26] Jain, A., and Rodriguez, G., 2003, "Multibody mass matrix sensitivity analysis using spatial operators," Int. J. for Multiscale Computational Engineering, 1 (2-3).
[27] Walker, M. W., and Orin, D. E., 1982, "Efficient dynamic computer simulation of robotic mechanisms," ASME J. of Dyn. Sys., Meas. and Control, vol. 104, pp. 205-211.
[28] Stejskal, V., and Valasek, M., 1996, Kinematics and Dynamics of Machinery, M. Dekkar Inc., New York.
[29] Jain, A., and Rodriguez, G., 1992, "Recursive flexible multibody system dynamics using spatial operators," Journal of Guidance, Controls and Dynamics, vol. 15, pp. 1453-1466.

APPENDIX A

Using the expressions for the total kinetic energy, $T = \sum_{i=1}^{n} T_i$, where T_i is given by eq. (17), the partial differentiations with respect to the set of j^{th} independent generalized speeds and coordinates, i.e., $\dot{\boldsymbol{q}}_j$ and $\boldsymbol{q}_j$, respectively, as required in eq. (20) are obtained as

$$\frac{\partial T}{\partial \dot{\boldsymbol{q}}_j} = \sum_{i=1}^{n}\left[\int_0^{b_i} \rho_i \dot{\boldsymbol{r}}_i^T \frac{\partial \dot{\boldsymbol{r}}_i}{\partial \dot{\boldsymbol{q}}_j}\, d\bar{b}_i + \int_0^{a_i} \rho_i \dot{\tilde{\boldsymbol{r}}}_i^T \frac{\partial \dot{\tilde{\boldsymbol{r}}}_i}{\partial \dot{\boldsymbol{q}}_j}\, d\bar{a}_i + m_{pi}\dot{\boldsymbol{r}}_{pi}^T \frac{\partial \dot{\boldsymbol{r}}_{pi}}{\partial \dot{\boldsymbol{q}}_j} + (\boldsymbol{I}_{hi}\boldsymbol{\omega}_i)^T \frac{\partial \boldsymbol{\omega}_i}{\partial \dot{\boldsymbol{q}}_j}\right] \tag{A.1a}$$

$$\frac{\partial T}{\partial \boldsymbol{q}_j} = \sum_{i=1}^{n}\left[\int_0^{b_i} \rho_i \dot{\boldsymbol{r}}_i^T \frac{\partial \dot{\boldsymbol{r}}_i}{\partial \boldsymbol{q}_j}\, d\bar{b}_i + \int_0^{a_i} \rho_i \dot{\tilde{\boldsymbol{r}}}_i^T \frac{\partial \dot{\tilde{\boldsymbol{r}}}_i}{\partial \boldsymbol{q}_j}\, d\bar{a}_i + m_{pi}\dot{\boldsymbol{r}}_{pi}^T \frac{\partial \dot{\boldsymbol{r}}_{pi}}{\partial \boldsymbol{q}_j} + (\boldsymbol{I}_{hi}\boldsymbol{\omega}_i)^T \frac{\partial \boldsymbol{\omega}_i}{\partial \boldsymbol{q}_j}\right] \tag{A.1b}$$

Next, $d/dt\left(\partial T/\partial \dot{\boldsymbol{q}}_j\right)$ is obtained from eq. (A.1a) as

$$\frac{d}{dt}\left(\frac{\partial T}{\partial \dot{\boldsymbol{q}}_j}\right) = \sum_{i=1}^{n}\left[\int_0^{b_i} \rho_i \left\{\ddot{\boldsymbol{r}}_i^T \frac{\partial \dot{\boldsymbol{r}}_i}{\partial \dot{\boldsymbol{q}}_j} + \dot{\boldsymbol{r}}_i^T \frac{d}{dt}\left(\frac{\partial \dot{\boldsymbol{r}}_i}{\partial \dot{\boldsymbol{q}}_j}\right)\right\} d\bar{b}_i + \int_0^{a_i} \rho_i \left\{\ddot{\tilde{\boldsymbol{r}}}_i^T \frac{\partial \dot{\tilde{\boldsymbol{r}}}_i}{\partial \dot{\boldsymbol{q}}_j} + \dot{\tilde{\boldsymbol{r}}}_i^T \frac{d}{dt}\left(\frac{\partial \dot{\tilde{\boldsymbol{r}}}_i}{\partial \dot{\boldsymbol{q}}_j}\right)\right\} d\bar{a}_i + m_{pi}\left\{\ddot{\boldsymbol{r}}_{pi}^T \frac{\partial \dot{\boldsymbol{r}}_{pi}}{\partial \dot{\boldsymbol{q}}_j} + \dot{\boldsymbol{r}}_{pi}^T \frac{d}{dt}\left(\frac{\partial \dot{\boldsymbol{r}}_{pi}}{\partial \dot{\boldsymbol{q}}_j}\right)\right\}$$

$$+\left\{(\boldsymbol{I}_{hi}\dot{\boldsymbol{\omega}}_i + \boldsymbol{\omega}_i \times \boldsymbol{I}_{hi}\boldsymbol{\omega}_i)^T \partial\boldsymbol{\omega}_i/\partial\dot{\boldsymbol{q}}_j + (\boldsymbol{I}_{hi}\boldsymbol{\omega}_i)^T d/dt\left(\partial\boldsymbol{\omega}_i/\partial\dot{\boldsymbol{q}}_j\right)\right\}\Bigg] \tag{A.2}$$

As shown in [28] and others, it is evident that

$$\partial\dot{\boldsymbol{r}}/\partial\dot{\boldsymbol{q}}_j = \partial\boldsymbol{r}/\partial\boldsymbol{q}_j \;;\; \partial\dot{\tilde{\boldsymbol{r}}}_i/\partial\dot{\boldsymbol{q}}_j = \partial\tilde{\boldsymbol{r}}_i/\partial\boldsymbol{q}_j \text{ and } \partial\dot{\boldsymbol{r}}_{pi}/\partial\dot{\boldsymbol{q}}_j = \partial\boldsymbol{r}_{pi}/\partial\boldsymbol{q}_j \tag{A.3}$$

Hence, the 2nd, 4th , 6th and 8th terms on the right hand side of eq. (A.2) are given by

$$\frac{d}{dt}\left(\frac{\partial \dot{\boldsymbol{r}}_i}{\partial \dot{\boldsymbol{q}}_j}\right) = \frac{d}{dt}\left(\frac{\partial \boldsymbol{r}_i}{\partial \boldsymbol{q}_j}\right) = \frac{\partial \dot{\boldsymbol{r}}_i}{\partial \boldsymbol{q}_j};\; \frac{d}{dt}\left(\frac{\partial \dot{\tilde{\boldsymbol{r}}}_i}{\partial \dot{\boldsymbol{q}}_j}\right) = \frac{d}{dt}\left(\frac{\partial \tilde{\boldsymbol{r}}_i}{\partial \boldsymbol{q}_j}\right) = \frac{\partial \dot{\tilde{\boldsymbol{r}}}_i}{\partial \boldsymbol{q}_j};\; \frac{d}{dt}\left(\frac{\partial \dot{\boldsymbol{r}}_{pi}}{\partial \dot{\boldsymbol{q}}_j}\right) = \frac{d}{dt}\left(\frac{\partial \boldsymbol{r}_{pi}}{\partial \boldsymbol{q}_j}\right) = \frac{\partial \dot{\boldsymbol{r}}_{pi}}{\partial \boldsymbol{q}_j} \text{ and } \frac{d}{dt}\left(\frac{\partial \boldsymbol{\omega}_i}{\partial \dot{\boldsymbol{q}}_j}\right) = \frac{\partial \boldsymbol{\omega}_i}{\partial \boldsymbol{q}_j} \tag{A.4}$$

Substituting eqs. (A.4) into eq. (A.2), and using the resulting expression, along with eq. (A.1b), the left hand side of eq. (20), is obtained as

$$\sum_{i=1}^{n}\left[\int_0^{b_i}\rho_i\,\ddot{\boldsymbol{r}}_i^{\,T}\frac{\partial\dot{\boldsymbol{r}}_i}{\partial\dot{\boldsymbol{q}}_j}\mathrm{d}\bar{b}_i+\int_0^{a_i}\rho_i\,\ddot{\tilde{\boldsymbol{r}}}_i^{\,T}\frac{\partial\dot{\tilde{\boldsymbol{r}}}_i}{\partial\dot{\boldsymbol{q}}_j}\mathrm{d}\bar{a}_i+m_{pi}\ddot{\boldsymbol{r}}_{pi}^{\,T}\frac{\partial\dot{\boldsymbol{r}}_{pi}}{\partial\dot{\boldsymbol{q}}_j}+(\boldsymbol{I}_{hi}\dot{\boldsymbol{\omega}}_i+\boldsymbol{\omega}_i\times\boldsymbol{I}_{hi}\boldsymbol{\omega}_i)\frac{\partial\boldsymbol{\omega}_i}{\partial\dot{\boldsymbol{q}}_j}\right]=\boldsymbol{\tau}_j \tag{A.5}$$

where cancellation of some terms happened. Next, from eq.(18b) and. (A.5), one obtains

$$\sum_{i=1}^{n}\left[\int_0^{b_i}\rho_i\left\{\ddot{\boldsymbol{r}}_i^{\,T}\frac{\partial\boldsymbol{v}_i}{\partial\dot{\boldsymbol{q}}_j}+\ddot{\boldsymbol{r}}_i^{\,T}\frac{\partial(\boldsymbol{\omega}_i\times\bar{b}_i\boldsymbol{z}_i)}{\partial\dot{\boldsymbol{q}}_j}\right\}\mathrm{d}\bar{b}_i+\int_0^{a_i}\rho_i\left\{\ddot{\tilde{\boldsymbol{r}}}_i^{\,T}\frac{\partial\boldsymbol{v}_i}{\partial\dot{\boldsymbol{q}}_j}+\ddot{\tilde{\boldsymbol{r}}}_i^{\,T}\frac{\partial[\boldsymbol{\omega}_i\times\bar{\boldsymbol{r}}_i+\dot{\boldsymbol{u}}_i]}{\partial\dot{\boldsymbol{q}}_j}\right\}\mathrm{d}\bar{a}_i+$$

$$m_{pi}\left\{\ddot{\boldsymbol{r}}_{pi}^{\,T}\frac{\partial\boldsymbol{v}_i}{\partial\dot{\boldsymbol{q}}_j}+\ddot{\boldsymbol{r}}_{pi}^{\,T}\frac{\partial[\boldsymbol{\omega}_i\times\bar{\boldsymbol{r}}_{pi}+\dot{\boldsymbol{u}}_{pi}]}{\partial\dot{\boldsymbol{q}}_j}\right\}+(\boldsymbol{I}_{hi}\dot{\boldsymbol{\omega}}_i+\boldsymbol{\omega}_i\times\boldsymbol{I}_{hi}\boldsymbol{\omega}_i)^T\frac{\partial\boldsymbol{\omega}_i}{\partial\dot{\boldsymbol{q}}_j}\right]=\boldsymbol{\tau}_j$$

Using the vector triple product rule [15], $\boldsymbol{a}^T(\boldsymbol{b}\times\boldsymbol{c})=(\boldsymbol{c}\times\boldsymbol{a})^T\boldsymbol{b}$ —$\boldsymbol{a}$, $\boldsymbol{b}$ and $\boldsymbol{c}$ are any 3-dimensional Cartesian vectors, one can show that

$$\ddot{\boldsymbol{r}}_i^{\,T}\frac{\partial(\boldsymbol{\omega}_i\times\bar{b}_i\boldsymbol{z}_i)}{\partial\dot{\boldsymbol{q}}_j}=\bar{b}_i\ddot{\boldsymbol{r}}_i^{\,T}\left(\frac{\partial\boldsymbol{\omega}_i}{\partial\dot{\boldsymbol{q}}_j}\times\boldsymbol{z}_i+\boldsymbol{\omega}_i\times\frac{\partial\boldsymbol{z}_i}{\partial\dot{\boldsymbol{q}}_j}\right)=\bar{b}_i(\boldsymbol{z}_i\times\ddot{\boldsymbol{r}}_i)^T\frac{\partial\boldsymbol{\omega}_i}{\partial\dot{\boldsymbol{q}}_j} \tag{A.6a}$$

$$\ddot{\tilde{\boldsymbol{r}}}_i^{\,T}\frac{\partial(\boldsymbol{\omega}_i\times\bar{\boldsymbol{r}}_i+\dot{\boldsymbol{u}}_i)}{\partial\dot{\boldsymbol{q}}_j}=\ddot{\tilde{\boldsymbol{r}}}_i^{\,T}\frac{\partial(\boldsymbol{\omega}_i\times\bar{\boldsymbol{r}}_i)}{\partial\dot{\boldsymbol{q}}_j}+\ddot{\tilde{\boldsymbol{r}}}_i^{\,T}\frac{\partial\dot{\boldsymbol{u}}_i}{\partial\dot{\boldsymbol{q}}_j}=\ddot{\tilde{\boldsymbol{r}}}_i^{\,T}\left(\frac{\partial\boldsymbol{\omega}_i}{\partial\dot{\boldsymbol{q}}_j}\times\bar{\boldsymbol{r}}_i+\boldsymbol{\omega}_i\times\frac{\partial\bar{\boldsymbol{r}}_i}{\partial\dot{\boldsymbol{q}}_j}\right)+\ddot{\tilde{\boldsymbol{r}}}_i^{\,T}\frac{\partial\dot{\boldsymbol{u}}_i}{\partial\dot{\boldsymbol{q}}_j}=(\bar{\boldsymbol{r}}_i\times\ddot{\tilde{\boldsymbol{r}}}_i)^T\frac{\partial\boldsymbol{\omega}_i}{\partial\dot{\boldsymbol{q}}_j}+\ddot{\tilde{\boldsymbol{r}}}_i^{\,T}\frac{\partial\dot{\boldsymbol{u}}_i}{\partial\dot{\boldsymbol{q}}_j} \tag{A.6b}$$

$$\ddot{\boldsymbol{r}}_{pi}^{\,T}\frac{\partial(\boldsymbol{\omega}_i\times\bar{\boldsymbol{r}}_{pi}+\dot{\boldsymbol{u}}_{pi})}{\partial\dot{\boldsymbol{q}}_j}=\ddot{\boldsymbol{r}}_{pi}^{\,T}\left(\frac{\partial\boldsymbol{\omega}_i}{\partial\dot{\boldsymbol{q}}_j}\times\bar{\boldsymbol{r}}_{pi}+\boldsymbol{\omega}_i\times\frac{\partial\bar{\boldsymbol{r}}_{pi}}{\partial\dot{\boldsymbol{q}}_j}\right)+\ddot{\boldsymbol{r}}_{pi}^{\,T}\frac{\partial\dot{\boldsymbol{u}}_{pi}}{\partial\dot{\boldsymbol{q}}_j}=(\bar{\boldsymbol{r}}_{pi}\times\ddot{\boldsymbol{r}}_{pi})^T\frac{\partial\boldsymbol{\omega}_i}{\partial\dot{\boldsymbol{q}}_j}+\ddot{\boldsymbol{r}}_{pi}^{\,T}\frac{\partial\dot{\boldsymbol{u}}_{pi}}{\partial\dot{\boldsymbol{q}}_j} \tag{A.6c}$$

In eqs. (A.6a-c), $\partial\boldsymbol{z}_i/\partial\dot{\boldsymbol{q}}_j=\boldsymbol{O}$, $\partial\bar{\boldsymbol{r}}_i/\partial\dot{\boldsymbol{q}}_j=\boldsymbol{O}$, and $\partial\bar{\boldsymbol{r}}_{pi}/\partial\dot{\boldsymbol{q}}_j=\boldsymbol{O}$ are used as $\boldsymbol{z}_i$, $\bar{\boldsymbol{r}}_i$ and $\bar{\boldsymbol{r}}_{pi}$ are functions of $\boldsymbol{q}_j$'s only, and not $\dot{\boldsymbol{q}}_j$'s. Moreover, using eq. (2e) and substituting $\dot{\boldsymbol{u}}_i=\boldsymbol{S}_i\dot{\boldsymbol{d}}_i$, along with $\dot{\boldsymbol{u}}_{pi}=\boldsymbol{S}_i|_{a_i}\dot{\boldsymbol{d}}_i$ in eqs. (A.6a-c), $\ddot{\tilde{\boldsymbol{r}}}_i^{\,T}\partial\dot{\boldsymbol{u}}_i/\partial\dot{\boldsymbol{q}}_j$ and $\ddot{\boldsymbol{r}}_{pi}^{\,T}\partial\dot{\boldsymbol{u}}_{pi}/\partial\dot{\boldsymbol{q}}_j$ are re-written as:

$$\ddot{\tilde{\boldsymbol{r}}}_i^{\,T}\frac{\partial\dot{\boldsymbol{u}}_i}{\partial\dot{\boldsymbol{q}}_j}=\ddot{\tilde{\boldsymbol{r}}}_i^{\,T}\boldsymbol{S}_i\frac{\partial\dot{\boldsymbol{d}}_i}{\partial\dot{\boldsymbol{q}}_j}\ \text{and}\ \ddot{\boldsymbol{r}}_{pi}^{\,T}\frac{\partial\dot{\boldsymbol{u}}_{pi}}{\partial\dot{\boldsymbol{q}}_j}=\ddot{\boldsymbol{r}}_{pi}^{\,T}\boldsymbol{S}_i|_{a_i}\frac{\partial\dot{\boldsymbol{d}}_i}{\partial\dot{\boldsymbol{q}}_j} \tag{A.7}$$

In eq. (A.7), $\boldsymbol{S}_i|_{a_i}$ is the shape function of the link evaluated at its tip, i.e., $\bar{a}_i=a_i$. Thus,

$$\sum_{i=1}^{n}\left[\int_0^{b_i}\rho_i\left\{\ddot{\boldsymbol{r}}_i^{\,T}\frac{\partial\boldsymbol{v}_i}{\partial\dot{\boldsymbol{q}}_j}+\bar{b}_i(\boldsymbol{z}_i\times\ddot{\boldsymbol{r}}_i)^T\frac{\partial\boldsymbol{\omega}_i}{\partial\dot{\boldsymbol{q}}_j}\right\}\mathrm{d}\bar{b}_i+\int_0^{a_i}\rho_i\left\{\ddot{\tilde{\boldsymbol{r}}}_i^{\,T}\frac{\partial\boldsymbol{v}_i}{\partial\dot{\boldsymbol{q}}_j}+(\bar{\boldsymbol{r}}_i\times\ddot{\tilde{\boldsymbol{r}}}_i)^T\frac{\partial\boldsymbol{\omega}_i}{\partial\dot{\boldsymbol{q}}_j}+\ddot{\tilde{\boldsymbol{r}}}_i^{\,T}\boldsymbol{S}_i\frac{\partial\dot{\boldsymbol{d}}_i}{\partial\dot{\boldsymbol{q}}_j}\right\}\mathrm{d}\bar{a}_i\right.$$

$$\left.+m_{pi}\left\{\ddot{\boldsymbol{r}}_{pi}^{\,T}\frac{\partial\boldsymbol{v}_i}{\partial\dot{\boldsymbol{q}}_j}+(\bar{\boldsymbol{r}}_{pi}\times\ddot{\boldsymbol{r}}_{pi})^T\frac{\partial\boldsymbol{\omega}_i}{\partial\dot{\boldsymbol{q}}_j}+\ddot{\boldsymbol{r}}_{pi}^{\,T}\boldsymbol{S}_i|_{a_i}\frac{\partial\dot{\boldsymbol{d}}_i}{\partial\dot{\boldsymbol{q}}_j}\right\}+(\boldsymbol{I}_{hi}\dot{\boldsymbol{\omega}}_i+\boldsymbol{\omega}_i\times\boldsymbol{I}_{hi}\boldsymbol{\omega}_i)^T\frac{\partial\boldsymbol{\omega}_i}{\partial\dot{\boldsymbol{q}}_j}\right]=\boldsymbol{\tau}_j \tag{A.8}$$

Now, introduce the following definitions:

$$\frac{\partial\boldsymbol{t}_i}{\partial\dot{\boldsymbol{q}}_j}\equiv\begin{bmatrix}\dfrac{\partial\boldsymbol{v}_i}{\partial\dot{\boldsymbol{q}}_j}\\[2mm]\dfrac{\partial\boldsymbol{\omega}_i}{\partial\dot{\boldsymbol{q}}_j}\\[2mm]\dfrac{\partial\dot{\boldsymbol{d}}_i}{\partial\dot{\boldsymbol{q}}_j}\end{bmatrix};\ \boldsymbol{w}_i^*\equiv\begin{bmatrix}\displaystyle\int_0^{b_i}\rho_i\,\ddot{\boldsymbol{r}}_i\mathrm{d}\bar{b}_i+\int_0^{a_i}\rho_i\,\ddot{\tilde{\boldsymbol{r}}}_i\mathrm{d}\bar{a}_i+m_{pi}\,\ddot{\boldsymbol{r}}_{pi}\\[2mm]\displaystyle\int_0^{b_i}\rho_i\,\bar{b}_i(\boldsymbol{z}_i\times\ddot{\boldsymbol{r}}_i)\mathrm{d}\bar{b}_i+\int_0^{a_i}\rho_i(\bar{\boldsymbol{r}}_i\times\ddot{\tilde{\boldsymbol{r}}}_i)\mathrm{d}\bar{a}_i+m_{pi}(\bar{\boldsymbol{r}}_{pi}\times\ddot{\boldsymbol{r}}_{pi})+(\boldsymbol{I}_{hi}\dot{\boldsymbol{\omega}}_i+\boldsymbol{\omega}_i\times\boldsymbol{I}_{hi}\boldsymbol{\omega}_i)\\[2mm]\displaystyle\int_0^{a_i}\rho_i\,S_i^T\ddot{\tilde{\boldsymbol{r}}}_i\mathrm{d}\bar{a}_i+m_{pi}\,S_i|_{a_i}^T\ddot{\boldsymbol{r}}_{pi}\end{bmatrix} \tag{A.9}$$

Then, eq. (A.8) is re-written in compact form as

$$\begin{bmatrix}\left(\dfrac{\partial\boldsymbol{t}_1}{\partial\dot{\boldsymbol{q}}_j}\right)^T & \cdots & \left(\dfrac{\partial\boldsymbol{t}_n}{\partial\dot{\boldsymbol{q}}_j}\right)^T\end{bmatrix}\begin{bmatrix}\boldsymbol{w}_1^*\\ \vdots\\ \boldsymbol{w}_n^*\end{bmatrix}=\boldsymbol{\tau}_j \tag{A.10}$$